SEMMELWEIS EGYETEM

DOKTORI ISKOLA

Ph.D. értekezések

3435.

TÓTH ÁKOS ROLAND

Gyermekkori betegségek klinikuma, élettana és prevenciója

című program

Programvezető: Dr. Szabó Attila, egyetemi tanár

Témavezető: Dr. Hosszú Ádám, tudományos munkatárs

Protective Effects of Sigma-1 Receptor Agonists in Renal Hypoxic Injury

PhD thesis

Ákos Roland Tóth

Semmelweis University Doctoral School

Rácz Károly Conservative Medicine Division

Supervisor:	Ádám Hosszú, Ph.D
Official reviewers:	Deján Dobi, MD, Ph.D
	Szilárd Kun MD, Ph.D
Head of the Complex Examination Committee:	Prof. László Szabó, MD, Ph.D
Members of the Complex Examination Committee:	Tamás Szabó, MD, Ph.D
	Orsolya Horváth, MD, Ph.D

Budapest

2026

Table of contents

List of abbreviations

AKI	Acute kidney injury
AKIN	Acute Kidney Injury Network
AKT	Protein Kinase B
AST	Aspartate aminotransferase
ATN	Acute tubular necrosis
ATP	Adenosine triphosphate
ATx	Autotransplantation
Bad	Bcl-2-associated death promoter
Bax	Bcl2-associated X, apoptosis regulator
BBB	Blood–brain barrier
Bcl-2	B-cell lymphoma 2
Bid	BH3-interacting domain death agonist
Bip	Binding immunoglobulin protein
BSA	Bovine serum albumin
BUN	Blood urea nitrogen
CI	Cold Ischemia
CKD	Chronic kidney disease
CNS	Central nervous system
DBD	Donation after brain death
DCD	Donation after circulatory death
DD	Deceased donor
DGF	Delayed graft function

ECD	Expanded criteria donation
eGFR	Estimated glomerular filtration rate
eNOS	endothelial nitric oxide synthase
ER	Endoplasmic reticulum
ERA	European Renal Association
ESRD	End stage renal disease
FDA	Food and Drug Administration
FLU	Fluvoxamine
GFR	Glomerular filtration rate
hERG	Human ether-a-go-go-related gene
HIF-1α	Hypoxia inducible factor 1-α
HK-2	Human kidney 2
HLA	Human leukocyte antigen
HMP	Hypothermic machine perfusion
HTK	Histidine-tryptophan-ketoglutarate
ICAM-1	Intercellular Adhesion Molecule-1
IFN-γ	Interferon gamma
IGFBP7	Insulin-like growth factor-binding protein 7
IL- 18	Interleukin-18
IRI	Ischemia/Reperfusion injury
JAK2	Janus kinase 2
KDIGO	Kidney Disease Improving Global Outcomes
KIM- 1	Kidney injury molecule-1

KRT	Kidney replacement therapy
KTx	Kidney transplantation
LD	Diving donor
LDH	Lactate dehydrogenase
L-FABP	Liver-type fatty acid-binding protein
LPS	Lipopolysaccharide
MAM	Mitochondrial-associated membranes
MAPKs	Mitogen-activated protein kinases
MCP-1	Monocyte chemoattractant protein 1
MTT	Methyl-thiazole tetrazolium
NFM	Non-fat dry milk
NF-κB	Nuclear factor κB
NGAL	Neutrophil-gelatinase-associated lipocalin
NMP	Normothermic machine perfusion
NO	nitric oxide
p53	Tumor protein 53
PAS	Periodic acid-Schiff
PBS	Phosphate-buffered saline
PI3K	Phosphoinositide-3-kinase
PSA	Polar surface area
RIFLE	Risk, Injury, Failure, Loss, and End-stage Kidney Disease
ROI	Regions of interest
ROS	Reactive oxygen species

RP-HPLC	Reversed-Phase High-Performance Liquid Chromatography
RRT	Renal Replacement Therapy
RT	Room temperature
RT-qPCR	Reverse transcription-quantitative polymerase chain reaction
S1R	Sigma-1 receptor
SCS	Static cold storage
SSRI	Selective serotonin reuptake inhibitors
STAT3	Signal transducer and activator of transcription 3
TdT	Terminal deoxynucleotidyl transferase
TIMP- 2	Tissue inhibitor of metalloproteinases-2
TLR 2	Toll-like receptor 2
TLR 4	Toll-like receptor 4
TNF-α	Tumor Necrosis Factor alpha
TUNEL	Terminal deoxynucleotidyl transferase dUTP nick end labeling
USRDS	United States Renal Data System
UW	University of Wisconsin
VCAM-1	Vascular Cell Adhesion Molecule-1

1. Introduction

1.1. End-stage renal disease

End-stage renal disease (ESRD) represents the final stage of chronic kidney disease (CKD) and is associated with complete loss of kidney function. ESRD stands as one of the leading causes of morbidity and mortality worldwide (1). The true incidence and prevalence of CKD are hard to determine due to its asymptomatic early stages, but it is estimated to impact over 10% of the general population, nearly 844 million people and increases with age (**Figure 1**) (2). Additionally, the incidence of ESRD is higher in males than in females (3).

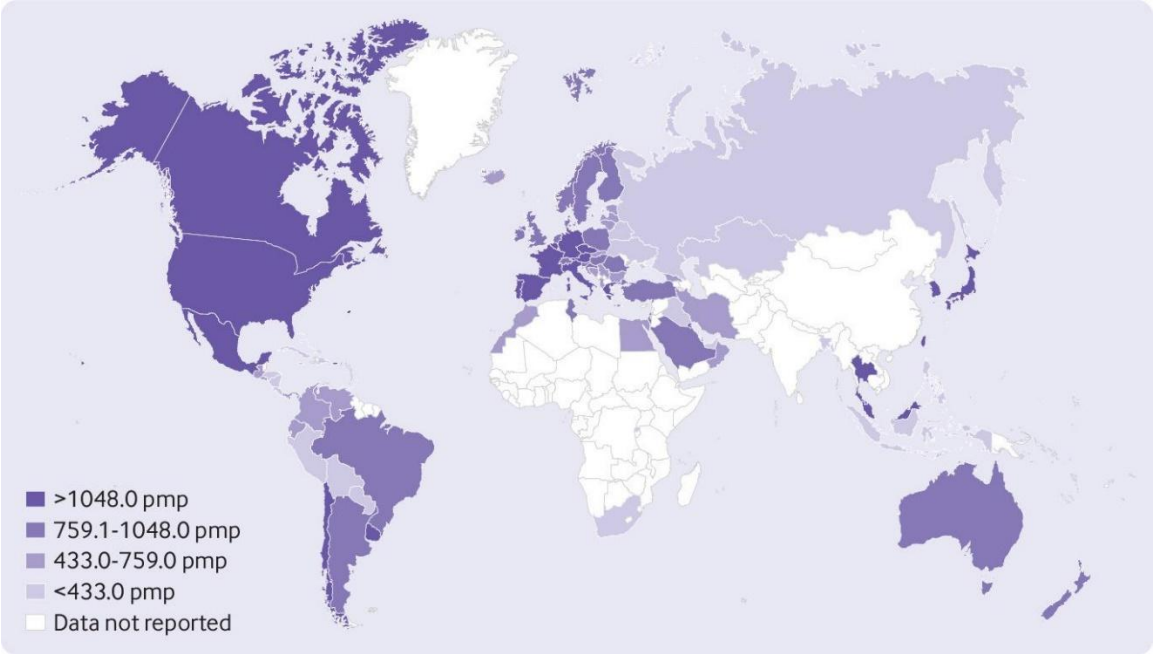

Figure 1. The estimated total number of treated end-stage renal disease (4).

Globally, the causes of CKD exhibit geographic variations, with lifestyle-related factors playing a significant role. In wealthy countries, the most common causes are noncommunicable diseases, such as diabetes mellitus (type I and II) in 30-50% of the cases and hypertension in 27% of the cases (5,6). In low- and middle-income countries, beyond diabetes and hypertension, infectious diseases and environmental toxins are responsible for CKD (7,8).

Importantly, acute kidney injury (AKI) is increasingly recognized as a key risk factor for CKD and ESRD, with individuals experiencing AKI facing a substantial, 9-fold

higher adjusted risk of progression to CKD, 3-fold higher risk of progressing to ESRD and mortality. Conversely, CKD also increases the risk of AKI, highlighting the bidirectional and interdependent relationship between the two conditions (9,10).

CKD is commonly identified through routine screening using serum chemistry profiles and urine analyses, with particular emphasis on estimating the glomerular filtration rate (eGFR) and assessing markers of kidney damage. The diagnostic criteria include a sustained eGFR below 60 mL/min/1.73 m² and/or evidence of structural or functional kidney damage. However, relying on a single parameter like eGFR has certain limitations: it reflects only renal function, is influenced by various non-renal factors, and changes with age in a non-linear manner (11). In response to these limitations, novel approaches such as the use of retinal imaging combined with artificial intelligence –based deep learning algorithms, like the RetiKid system, are being explored to enable earlier and potentially more accurate diagnosis of CKD (12,13).

Kidney replacement therapies (KRTs) are essential interventions for patients with ESRD. The prevalence of KRT increased 2.4% in Europe and 2.8% in US annually between 2012 and 2019. The primary KRT modalities include hemodialysis, peritoneal dialysis with 78% and kidney transplantation (KTx) with 22% (14). In Hungary this ratio is 64% dialysis and 36% is KTx (15,16).

Dialysis, either peritoneal or hemodialysis, remains a vital option for patients who are not suitable candidates for KTx or who are awaiting a donor organ. However, it comes with several side effects including cardiovascular and metabolic risks. Moreover, access to dialysis centers is not universally available, particularly in remote or underserved regions, and patient transportation can pose logistical challenges (17). Moreover, dialysis imposes a significant financial burden (18). In the European Union, the average annual cost per dialysis patient is around €80,000 (19). In contrast, KTx offers a more cost-effective solution. In Eastern and Central Europe, the median first-year cost of KTx is approximately €45,000, which is significantly lower than the annual costs associated with dialysis (20).

1.2. Kidney transplantation

KTx remains the gold standard treatment for improving both survival and quality of life in patients with ESRD (21). Over the past decade, transplantation rates have increased annually by 1.9% in Europe and 4.3% in the United States for both deceased and living donor transplants (**Figure 2**). Despite the well-established superior outcomes associated with living donor kidney transplantation—including improved graft survival and function—deceased donors still account for the majority of transplants in both Europe (78%) including Hungary (81%) and the US (77%) (**Figure 3**) (22). Most deceased kidney donors are classified as donation after brain death (DBD), characterized by irreversible loss of brainstem function, while about one-third are from donation after circulatory death (DCD). Another source of donor organs is expanded criteria donation (ECD), which encompasses DCD as well as those with specific comorbidities, such as arterial hypertension or age over 60 years (23).

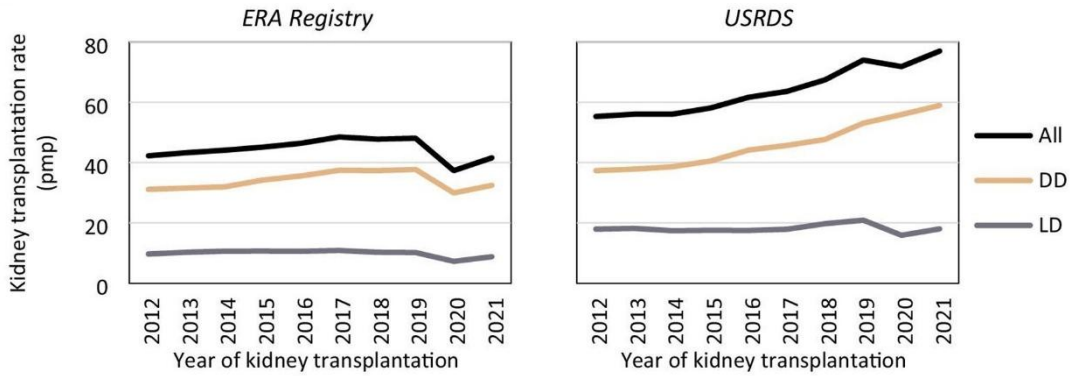

Figure 2. Trends over time in the kidney transplantation rate per million population for the ERA Registry and the USRDS, overall and by donor type. DD: deceased donor; LD: living donor; pmp: per million population (modified image of Stel et al. 2024) (14).

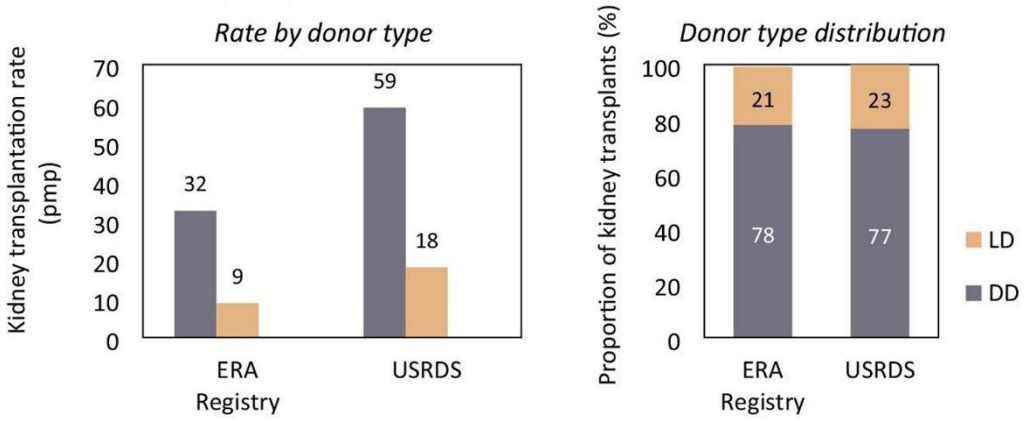

Figure 3. The incidence of KRT in the kidney transplantation as a rate per million population or per 1000 patients DD: deceased donor; LD: living donor; pmp: per million population. (modified image of Stel et al. 2024)(14)

The advantages of living donor transplants are largely attributed to reduced cold ischemia (CI) time, better human leukocyte antigen (HLA) matching, and the ability to plan the procedure electively under optimal conditions (24). Significant advancements in surgical techniques, immunosuppressive regimens, and post-transplant monitoring have resulted in excellent short-term outcomes, with one-year graft survival now exceeding 95% (25). Nevertheless, these short-term improvements have yet to be matched by equivalent gains in long-term graft longevity, in which renal graft ischemia/reperfusion injury (IRI) is one of the critical factors (24).

In transplantation, renal grafts undergo ischemia at multiple stages—CI during procurement and static preservation, and warm ischemia during extraction and vascular anastomosis (26). There is evidence that prolonged cold ischemic time increases risk of delayed graft function (DGF), which can negatively impact long-term graft survival, in both deceased and living donor transplantation as well (27).

Several new strategies shown promising results to mitigate cold ischemic injury (**Figure 4**). In clinical practice two methods of organ preservation is used: static cold storage (SCS) and machine perfusion. During SCS the donor kidney is perfused with preservation solution immediately after retrieval and stored in it at 4°C until transplantation (28). Several preservation solutions are in clinical use worldwide, with the most common being the University of Wisconsin (UW) solution, histidine-

tryptophan-ketoglutarate (HTK) and Celsior (29). All these solutions showed similar risk of DGF and graft loss (30). In contrast, machine perfusion techniques offer dynamic preservation. Hypothermic machine perfusion (HMP) circulates oxygenated preservation solution through the kidney at low temperatures (4–10°C), with defined pressure, which reduces metabolic activity, mediates hypoxia-related gene and pro-inflammatory cytokine expression, and improves graft viability (31,32). More recently, normothermic machine perfusion (NMP) has emerged, maintaining the organ at near-physiological temperatures (35–37°C) with an oxygenated blood-based solution to support metabolic activity and organ function (33). Each of these methods represents an advancement toward reducing cold ischemic injury.

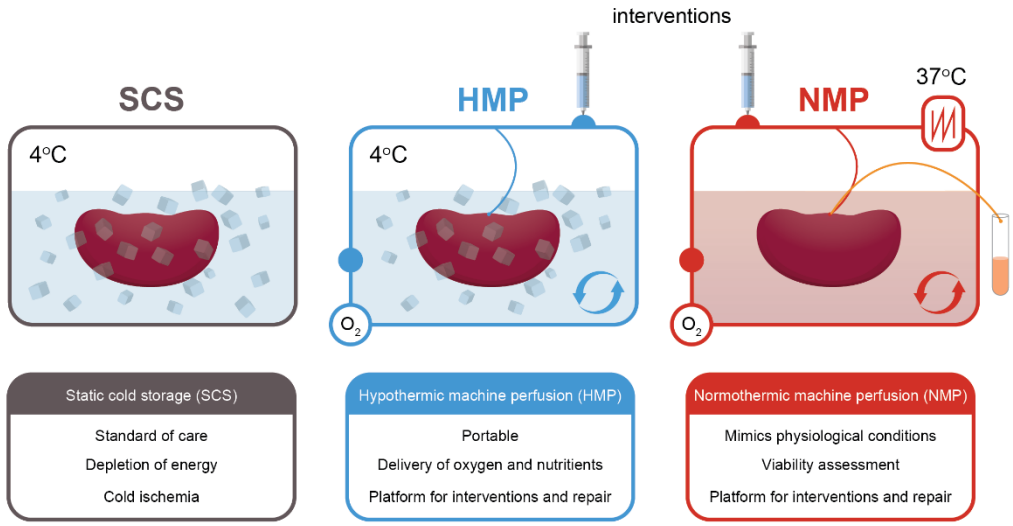

Figure 4. Current strategies for maintaining donor kidney viability prior to transplantation (modified image of van Leeuwen et al. 2022)(33)

1.3. Acute kidney injury

AKI is a clinical condition defined by an abrupt loss of kidney function which is determined by increased serum creatinine and reduced urinary output levels, leading to the accumulation of metabolic waste products, electrolyte imbalances, and disturbances in fluid homeostasis (34). Rather than being a single disease, AKI is a syndrome with diverse etiologies (35). In high-income countries, AKI is predominantly hospital-acquired, often affecting older patients with multiple comorbidities (36). In these cases,

AKI is primarily caused by diabetes mellitus, cardiovascular disease, post-surgical complications, or other iatrogenic factors. However, in low-income countries, community-acquired AKI is more prevalent and arises from dehydration, infections, sepsis, toxin exposure, and pregnancy-related complications. Here, patients are typically younger and face significant challenges to accessing healthcare (37). The pooled average mortality rate for AKI is 23% in high-income countries but rises significantly to 42% in low-income countries (38).

Diagnosing AKI can be challenging as clinical signs are often subtle or entirely absent. Kidney function loss is typically identified by increases in serum creatinine levels, but oliguria and anuria can also be primary indicators (39). In the mid-2000s, RIFLE (Risk, Injury, Failure, Loss, and End-stage Kidney Disease) and AKIN (Acute Kidney Injury Network) classifications were introduced to standardize the definition of AKI (40). RIFLE focused on changes in serum creatinine, glomerular filtration rate (GFR), and urine output to stratify the severity of AKI (41). AKIN built upon RIFLE by refining diagnostic criteria, such as incorporating smaller changes in serum creatinine over shorter time frames. Both classifications had limitations, like inconsistent application and limited prognostic accuracy across diverse populations (42). Nowadays, the KDIGO (Kidney Disease Improving Global Outcomes) classification is used in clinical practice and research, integrating and enhancing earlier systems to offer superior diagnostic and prognostic accuracy (**Table 1**) (43).

Table 1. KDIGO classification, diagnosis of acute kidney injury (AKI). eGFR: Estimated glomerular filtration rate; RRT: Renal Replacement Therapy

Stage	Serum creatinine level	Urine output
Diagnosis	▪increase of ≥ 0.3mg/dl (26.5µmol/l) within 48 h, or ▪increase of ≥ 1.5 fold above baseline, known or assumed to have occurred within 7 days	▪ < 0.5 ml/kg/h for 6 h
1	▪ ≥ 1.5-1.9 times baseline, or ▪> 0.3 mg/dl (26.5µmol/l) increase from baseline	▪ < 0.5 ml/kg/h for 6 - 12 h
2	▪ ≥ 2.0- 2.9 times baseline	▪ < 0.5 ml/kg/h for ≥ 12 h
3	▪ ≥ 3.0 times baseline ▪increase serum creatinine to ≥ 4.0 mg/dl (353,6 µmol/l), or ▪RRT or ▪in patient aged < 18 years, a decrease in eGFR to < 35ml/min/1.73m2	▪ < 0.3 ml/kg/h for ≥ 24 h or ▪ anuria for ≥ 12 h

Over the past decade, the diagnosis of AKI has evolved significantly, transitioning from reliance on clinical and biochemical markers to molecular-level (44). This advancement includes the identification and Food and Drug Administration (FDA)

approval of novel biomarkers for tubular injury, which enhance early diagnosis, stratify injury severity, and improve predictions of patient outcomes (45). Kidney injury molecule-1 (KIM-1), a type 1 transmembrane protein, is significantly upregulated in the proximal tubule following ischemic or nephrotoxic injury (46). It is a sensitive early biomarker, detectable in urine within the first hour of kidney injury, well before changes in serum creatinine levels (47). Urinary KIM-1 specifically reflects proximal tubular damage and predicts AKI outcomes in patients undergoing cardiac surgery (48). Neutrophil-gelatinase-associated lipocalin (NGAL) is produced mostly in epithelial cells of distal tubules but can also be found in proximal tubules. NGAL levels are typically low in healthy individuals, but increases massively 3 hours after an ischemic AKI in urine (49). Different studies showed NGAL as a predictor of AKI in critically ill, cardiac surgery, trauma, and sepsis patients (50,51). Additionally, both KIM-1 and NGAL are strong indicators for assessing the risk of progression from AKI to CKD (48,52).

Several other biomarkers showed promising results enhancing early detection of AKI. Interleukin-18 (IL-18), a pro-inflammatory cytokine, is rapidly elevated in the urine following ischemic kidney injury, reflecting early tubular damage (53). Tissue inhibitor of metalloproteinases-2 (TIMP-2) and insulin-like growth factor-binding protein 7 (IGFBP7) are stress-response proteins that predict cellular cycle arrest in renal tubular cells, making them effective markers for identifying patients at risk of AKI (54,55). Liver-type fatty acid-binding protein (L-FABP), another novel biomarker, is released from the proximal tubules under ischemic or oxidative stress conditions and is detectable in urine, providing insights into tubular injury and prognosis (56). Although these biomarkers show significant potential for early AKI diagnosis, they are not yet incorporated into routine clinical practice. Serum creatinine and urine output remain the gold standard for AKI diagnosis due to their established utility and widespread accessibility (57).

Renal histological changes offer specific and valuable insights into the pathophysiology of AKI, aiding in its diagnosis. Acute tubular injury can affect both proximal and distal tubules, manifesting as focal or diffuse tubular lumen dilation, loss of the brush border in proximal tubules, simplification of the tubular epithelium, and nuclear loss. Additionally, acute tubular necrosis (ATN), often associated with ischemic injury, may be observed in histological samples as well (**Figure 5**). This condition is

characterized by focal or diffuse coagulative-type necrosis of tubular epithelial cells and their detachment from the basement membrane (58).

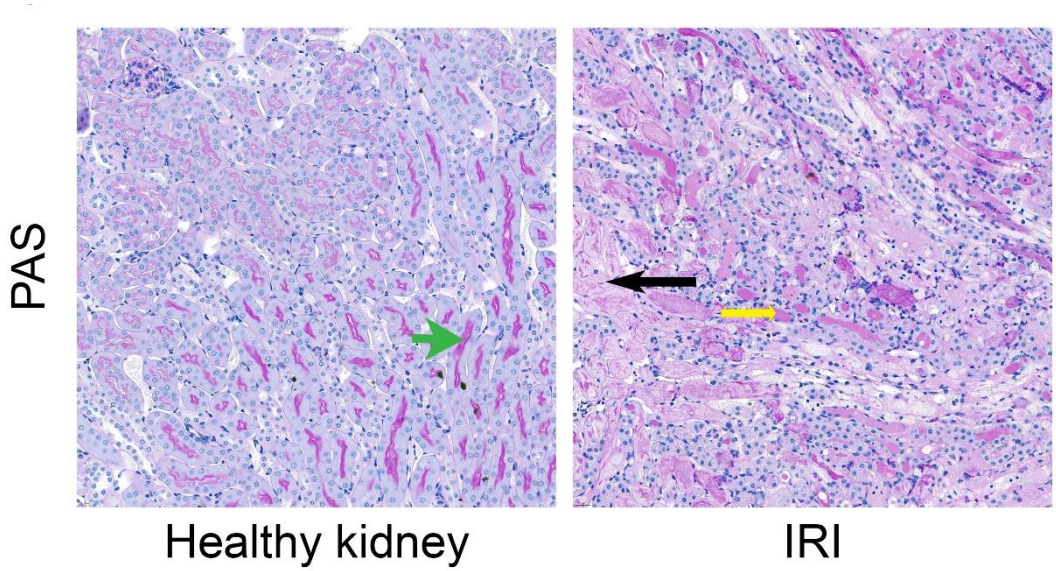

Figure 5. Representative periodic acid-Schiff stained sections of control and post-ischemic mice kidneys. Green arrow points to intact brush border; yellow arrow shows hyalin accumulation; black arrow shows necrotic tubule.

1.4. Ischemia/Reperfusion injury (IRI)

IRI is a major contributor to AKI and an unavoidable event in renal transplantation. It occurs when blood supply to the kidneys is temporarily reduced, followed by restoration and reoxygenation (59). The resulting oxygen deprivation forces epithelial cells to shift from aerobic to anaerobic metabolism, leading to reduced adenosine triphosphate (ATP) production and intracellular acidosis (60).

On the molecular level ischemia destabiliz

es lysosomal membranes, resulting in the leakage of lysosomal enzymes and cytoskeletal degradation. Inhibition of Na^+/K^+ ATPase leads to intracellular Na^+ and water accumulation, causing cellular edema. ATP depletion leads to intracellular Ca^{2+} overload, hypoxanthine accumulation, fueling reactive oxygen species (ROS) production upon reperfusion(61–63). RNA sequencing studies revealed that ischemia enriched metabolism-related pathways, including melatonin/serotonin degradation, lipid metabolism, bupropion/acetone degradation, and estrogen biosynthesis. It also enhanced pathways associated with apoptosis, fibrosis, and adipogenesis (64).

The ischemic phase primarily reduces capillary blood flow, while reperfusion exacerbates endothelial injury. The rapid restoration of oxygen supply triggers an excessive production of ROS, driven by mitochondrial dysfunction and the reverse action of complex I in the electron transport chain due to accumulated succinate. This oxidative burst leads to lipid peroxidation, mitochondrial permeability transition pore opening, and cytochrome C release, triggering apoptosis and necrosis. Intracellular Ca^{2+} overload further activates calpains, compromising cell integrity. Endothelial damage is worsened by vasoconstrictors like endothelin and leukocyte adhesion, leading to increased permeability and inflammation. ROS- activated neutrophils and platelets release oxidants and inflammatory mediators, creating a cycle of interstitial edema, inflammation, and microvascular dysfunction, ultimately worsening renal injury(60,65).

Ischemia, along with vasoconstriction and vessel occlusion, reduces oxygen delivery, leading to tubular cell injury. In nephron segments such as the S3 segment of the proximal tubule, epithelial cells experience relative hypoxia even under normal conditions due to restricted blood flow and oxygen exchange (66). With their high metabolic demands and limited capacity for anaerobic energy production, they are particularly vulnerable to ischemic damage. During ischemia, ATP depletion disrupts essential cellular functions, leading to apical brush border loss in proximal tubular epithelial cells, cytoskeletal destabilization, increased permeability, and epithelial detachment from the tubular basement membrane (67,68). These changes contribute to proximal tubular dilation, distal tubule cast formation, and obstruction of renal microcirculation, further exacerbating kidney damage (69). As a result, some tubular cells undergo apoptosis and necrosis.

Inflammation in IRI pathophysiology is complex and involves both innate and adaptive immunity (70). The innate immune response is initiated by endothelial and tubular epithelial cell injury, leading to the release of damage-associated molecular patterns that activate toll-like receptors, such as Toll-like receptor 2 (TLR2) and Toll-like receptor (TLR4), thereby triggering inflammatory cascades (71). Additionally, IRI leads to endothelial cell activation by upregulating adhesion molecules (E-selectin, P-selectin, ICAM-1, VCAM-1) that promote leukocyte infiltration (72,73). Neutrophils, as first responders, exacerbate injury by blocking renal microvessels, producing ROS, and secreting proteases, while monocytes differentiate into pro-inflammatory M1

macrophages, further amplifying cytokine release (Tumor Necrosis Factor alpha (TNF-α), IL-6, IL-8, IL-12, IL-1β) and inducing apoptosis to promote the inflammatory cascade, worsening tissue damage (74–76). The adaptive immune response activates when antigen-presenting cells, like dendritic cells and B cells stimulate T cells. Tubular epithelial cells enhance this by expressing costimulatory molecules. CD4+ T helper cells amplify inflammation, interferon gamma (IFN-γ) and TNF-α, while cytotoxic CD8+ T cells cause direct injury (60).

Apoptosis is a highly regulated and controlled process in renal IRI, in which the caspase family of proteases is responsible for self-limiting programmed cell death. There are two pathways that occur in apoptosis. In the intrinsic pathway, there is an increase in the permeability of the mitochondrial membrane, resulting in the leakage of apoptotic proteins due to the actions of Bcl2-associated X, apoptosis regulator (Bax) and Bcl-2-associated death promoter (Bad). In contrast, the extrinsic pathway is triggered by disturbances in the extracellular microenvironment mediated by caspase-8 (69). Both pathways activate the final enzymatic cascades of apoptosis through caspase-3 (77). The balance between proapoptotic (Bax, Bad, Bid) and antiapoptotic (B-cell lymphoma 2 (Bcl-2), Bcl-xL) Bcl-2 family proteins regulates intrinsic apoptosis, with renal IRI shifting this balance toward cell death by increasing Bax and decreasing Bcl-2. Nuclear factor κB (NF-κB) and Tumor protein 53 (p53) also contribute to the regulation of apoptosis (68,69).

1.5. Sigma-1 receptor

The Sigma-1 receptor (S1R) is a 25 kDa ligand-regulated chaperone protein encoded by the *SIGMAR1* gene, with a distinct structure compared to other mammalian proteins (78). The canonical Sig-1R isoform consists of 223 amino acids and features an N-terminal region with an endoplasmic reticulum (ER) retention signal, while the C-terminal domain shares similarities with steroid-binding regions (**Figure 6**) (79).

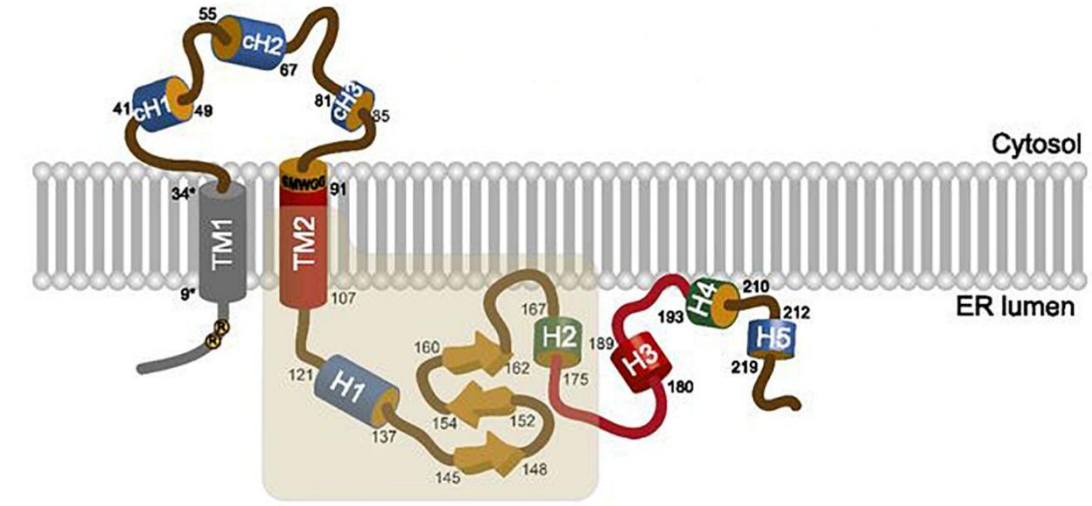

Figure 6. Structure of the Sigma-1 receptor. cH: cytosolic helic; ER: endoplasmic reticulum; TM1: transmembrane helix 1; TM2: transmembrane helix 2, H: helix; (modified image of Uyen B. et al. 2016)(80)

It is primarily expressed in the central nervous system (CNS); however, it can also be detected in peripheral tissues, including the liver, kidneys, lungs, heart, and muscles (81,82). S1R is intracellularly located in the specific microdomains of the ER, called mitochondrial-associated membranes (MAM), but this can depend on the cell type (83). Under normal conditions, S1R forms an inert complex with the main ER chaperone binding immunoglobulin protein (BiP). However, ligand activation leads to separation from BiP, after which S1R can relocate from MAM to the plasma membrane or nucleus, where it interacts with various nuclear factors to influence gene transcription. S1R interacts with a range of structurally diverse ligands, which may act as either agonists or antagonists, thereby inducing distinct cellular responses depending on the type of ligand bound. S1R antagonists inhibit the dissociation of S1R from BiP, thereby preventing S1R activation, while agonists, along with reduced calcium levels, facilitate the release of BiP from S1R, initiating downstream signaling pathways (84,85).

S1R is involved in numerous brain functions, including the regulation of cognition, memory, motor activity, sensory processing, pain modulation, and psychiatric behaviors. Additionally, S1R influences substance use and addiction, playing a role in the regulation of drug and alcohol consumption. The receptor has also been associated with neurodegenerative diseases like Alzheimer’s disease, Parkinson’s disease, and

Huntington's disease. Studies have demonstrated that the S1R plays a role in the brain injury response, with increased expression observed in the peri-infarct regions, suggesting its potential as a biomarker and therapeutic target in ischemic stroke (85,86).

The S1R plays various roles on the molecular level, influencing various physiological and pharmacological processes. At the plasma membrane, S1R interacts with ion channels (sodium, potassium, calcium, and chloride), receptor tyrosine kinases, G protein-coupled receptors, and integrins to regulate their activities and initiate intracellular signaling cascades. These interactions enable S1R to mediate complex cellular responses. Within the ER, S1R contributes significantly to oxidative stress regulation by coordinating calcium signaling between the ER and mitochondria via inositol 1,4,5-trisphosphate receptors. This cross-talk is essential for maintaining cellular energy balance and reducing oxidative damage (87). Moreover, S1R signaling exhibits protective anti-apoptotic effects through the modulation of several critical pathways, including the regulation of Bax and Bcl-2 levels, caspase-3 activity, and the activation of mitogen-activated protein kinases (MAPKs), phosphoinositide-3-kinase (PI3K)/ Protein Kinase B (AKT) signaling, p53, and the hypoxia-inducible factor 1 alpha (HIF-1α) pathways (88).

Interestingly, selective serotonin reuptake inhibitors (SSRIs)—widely used in treating anxiety, obsessive-compulsive disorder, and other neuropsychiatric conditions may act, in part, through S1R. SSRIs, such as fluvoxamine (FLU), with high affinity for S1R (Ki = 17.0 nM), appear to engage the receptor, suggesting a role for S1R in their mechanisms of action. Notably, S1R activation with agonists has shown protective effects in both neuropsychiatric and neurodegenerative disorders, also treatment with S1R agonists can mitigate infarct areas, likely by enhancing cell survival, and moderating inflammatory responses (89,90).

Peripheral organ studies underscore S1R modulation as a promising therapeutic target, particularly for its significant cardioprotective effects. In the heart, S1R activation helps to mitigate myocardial apoptosis by upregulating anti-apoptotic Bcl-2 and downregulating Bax and caspase-3, thus reducing susceptibility to ventricular arrhythmias (91,92). Additionally, S1R signaling promotes angiogenesis through activation of the Janus kinase 2 (JAK2)/signal transducer and activator of transcription 3 (STAT3) pathway (93). The S1R agonist PRE-084 has also been shown to enhance

cardioprotection by increasing phosphorylation of AKT and endothelial nitric oxide synthase (eNOS), emphasizing the importance of the AKT/eNOS pathway in maintaining cardiac function and resilience (87).

In the kidneys, S1R plays a similarly protective role, with its expression primarily localized in the renal cortex, especially in proximal tubules, with lesser expression in the medulla and papilla (94). Recent studies show increased S1R expression in distal tubular kidney cells of young and streptozotocin-induced diabetic rats(95). In a preclinical rat IRI model, we showed that activating the S1R with its natural ligand, the sex hormone 17β-estradiol, may lead to enhanced recovery outcomes in females following renal IRI (96). Furthermore, we demonstrated that S1R agonist FLU treatment improved post-ischemic damage by promoting AKT-mediated nitric oxide (NO) signaling, leading to better survival and preservation of renal structure and function (94).

2. Objectives

First, our aim was to assess whether pretransplant perfusion and cold storage of donor kidneys with S1R agonist FLU improves transplant outcomes by attenuating ischemic injury.

Next, we aimed to develop a novel S1R agonist with limited blood–brain barrier (BBB) penetration and to evaluate its efficacy in mitigating ischemic injury.

Furthermore, we aimed to investigate key inflammatory and apoptotic molecular pathways involved in IRI and to examine how S1R activation modulates these responses.

The following objectives have been set to fulfill the aims:

1. To investigate the renoprotection exerted by FLU in a rat model of KTx
2. To investigate whether organ preservation time can be lengthened, and pre-transplant graft condition can be improved with FLU in an *ex vivo* CI model
3. To develop a new S1R agonist with limited BBB penetration to avoid CNS side effects
4. To evaluate the renoprotective effect of the newly developed S1R agonist 'VCC904125' in a mouse model of renal IRI
5. To demonstrate that supplementing the preservation fluid with VCC904125 is renoprotective in an *ex vivo* CI model
6. To determine whether the observed renoprotective effects are mediated by S1R by assessing the effects of S1R agonists in S1R knockout mice.
7. To investigate the anti-inflammatory and anti-apoptotic molecular mechanisms of S1R activation

3. Methods

Animals

The following animals were used in all experiments: 6-week old male Han Wistar rats (Toxi-Coop Ltd., Budapest, Hungary); 6-8-week old C57BL/6J mice (Animalab Kft, Budapest, Hungary); or wild-type ($S1R^{+/+}$) and S1R-knockout ($S1R^{-/-}$) mice of a C57BL/6J × 129 s/Sv mixed background bred in our animal facility. The $S1R^{-/-}$ and $S1R^{+/+}$ genotypes were confirmed by PCR. Animals were housed in standard laboratory cages and were kept in standard conditions with a 12-hour dark/light cycle with free access to rodent chow and water. Animal procedures were approved by the Committee on the Care of Laboratory Animals at Semmelweis University, Budapest, Hungary (PEI/001/1731-9-2015).

Kidney isograft autotransplantation (ATx) model

Rats (n=8/group) were randomly assigned to the following groups: (i) Sham-operated controls; (ii) left kidney perfused with Custodiol (ATx); (iii) left kidney perfused with Custodiol + 10 μM FLU (ATx FLU). Rats were anesthetized with ketamine (75 mg × $bwkg^{-1}$, Richter Gedeon Plc., Budapest, Hungary) and xylazine (10 mg × $bwkg^{-1}$, Medicus Partner, Biatorbagy, Hungary). Renal autotransplantation was performed as follows: the kidneys and vessels were reached through a midline incision, and atraumatic vascular clips were applied to the left renal artery and vein. Left kidney was removed and perfused with ice cold (i) Custodiol (Na^+ : 15 mmol/L; K^+ : 9 mmol/L; Mg^{2+} : 4 mmol/L; Ca^{2+} : 0.015 mmol/L; histidine: 198 mmol/L; tryptophan: 2 mmol/L; ketoglutarate: 1 mmol/L; mannitol: 30 mmol/L) (Franz Kohler Chemie GMBH, Bensheim, Germany) or Custodiol containing 10 μM FLU. After 2 h of static cold storage in the same solution, the kidney was placed back into the same rat, and end-to-end anastomosis of the renal artery, vein, and ureter was performed. At the end of the 35-minute warm ischemia time, reperfusion was visually confirmed, and the contralateral kidney was removed. Twenty-four hours after reperfusion, blood samples were collected and centrifuged, and the sera were immediately snap-frozen. The kidneys were harvested and instantly snap-frozen in liquid nitrogen or fixed in 4% buffered paraformaldehyde (pH 7.4) for further investigation.

Renal ischemia/reperfusion (IRI) injury model

6-week-old male C57BL/6J mice (n=7-8/group) were pretreated *ip*. as follows: (i) isotonic saline as vehicle (IRI); or (ii) 20 mg x $bwkg^{-1}$ VCC904125 (IRI VCC). General anesthesia was induced by intraperitoneal administration of ketamine (90 mg × $bwkg^{-1}$) and xylazine (10 mg × $bwkg^{-1}$). The kidneys and vessels were accessed through a midline incision, and renal ischemia was achieved by clamping the left renal pedicles for 25 minutes with an atraumatic vascular clamp. Ischemia was visually confirmed. Before the ischemic phase concluded, the contralateral kidney was removed, then the vascular clips were released, and reperfusion was visually confirmed. Sham animals received similar surgical procedures without clamping. Twenty-four hours after reperfusion, mice were reanesthetized and euthanized by exsanguination. Blood samples were collected and centrifuged, and sera were immediately snap-frozen. Kidney tissue samples were collected and immediately snap-frozen in liquid nitrogen or fixed in 4% buffered paraformaldehyde (pH 7.4) for further investigation.

Cold ischemia (CI) model

The rats were randomly divided into following groups: (**1**) Control (**2**) Custodiol 2 h of cold ischemia (2h CI); (**3)** Custodiol + 10 µM FLU 2 h of CI (2h CI+ FLU); (**4**) Custodiol + 10 µM FLU 24h of CI (24h CI+ FLU).

The mice were randomly assigned to following groups: (**1**) Control; (**2**) wild-type Custodiol 24h of CI ($S1R^{+/+}$ 24h CI); (**3**) wild-type Custodiol + 10 µM FLU 24h of CI ($S1R^{+/+}$ 24h CI FLU); (**4**) S1R knockout Custodiol + 10 µM FLU 24h of CI ($S1R^{-/-}$ 24h CI FLU); (**5**) Custodiol+ 10 µM VCC 24h of CI (CI 24h Cust+ VCC).

General anesthesia was induced by intraperitoneal administration of ketamine (90 mg × $bwkg^{-1}$) and xylazine (10 mg × $bwkg^{-1}$). The renal artery and vein were isolated, and the kidneys were flushed with 4 °C isotonic saline for 1 min. Next, the kidneys were perfused with 200 mL of 4 °C Custodiol or Custodiol + S1R agonist at a perfusion pressure of 80–100 mmHg. The perfusion was considered complete when all blood had been removed from the kidney, as confirmed by visual control. The kidneys were placed in the same preservation solution and stored on ice for 2 or 24 h; to ensure stable temperature conditions, the containers holding the kidneys were kept in a refrigerator at

4 °C throughout the storage period. This was followed by fixation in 4% buffered paraformaldehyde (pH 7.4) for further investigation.

Measurement of renal function

Blood samples were centrifuged at room temperature for 6 min at 3600 rpm, and sera were collected and stored at -80°C. Serum creatinine, blood urea nitrogen (BUN), aspartate aminotransferase (AST), and serum electrolyte (sodium, potassium, chloride) levels were analyzed. The measurements were performed using a Beckman Coulter analyzer (Beckman Coulter, Brea, CA).

Synthesis of VCC904125

The VCC904125 compound (MW = 346.35 Da) was synthesized in five chemical steps, as presented in **Figure 7**:

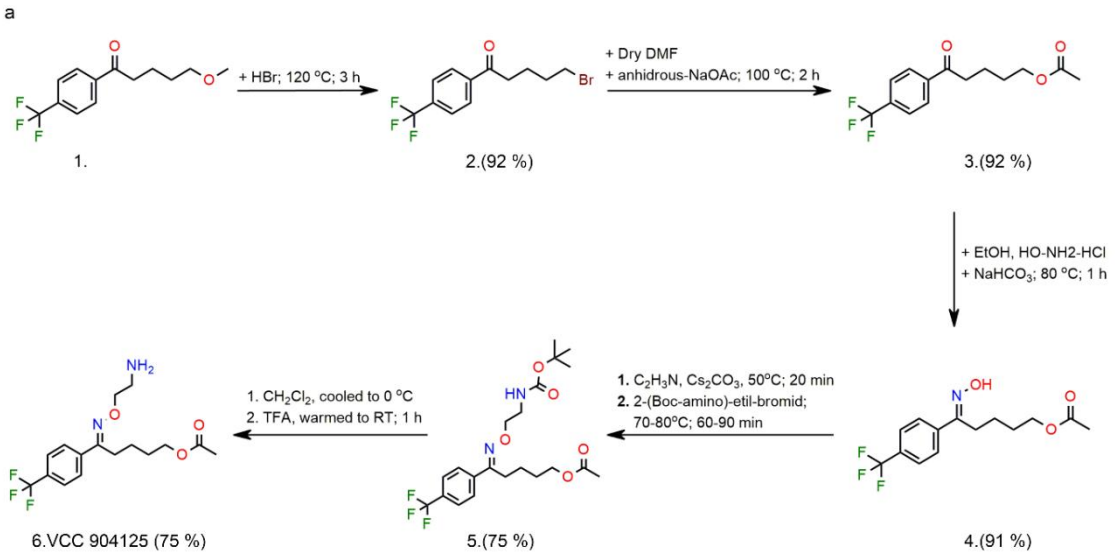

Figure 7. Synthesis route of the VCC904125 compound. a Synthesis route of the VCC904125 ((**1**) 5-methoxy-1-[4-(trifluoromethyl) phenyl] pentan-1-one; (**2**) 5-bromo-1- [4 (trifluoromethyl) phenyl] pentan-1-one; (**3**) 5-oxo-5-[4-(trifluoromethyl) phenyl] pentyl acetate; (**4**) (5E) -5-(hydroxyimino)-5-[4-(trifluoromethyl) phenyl] pentyl acetate;

(**5**) (5E)-13,13-dimethyl-11-oxo-5-[4-(trifluoromethyl) phenyl]-7,12-dioxa-6,10-diazatetradec-5-en-1-yl acetate; (**6**) (5E)-5-[(2-aminoethoxy)imino]-5-[4-(trifluoromethyl) phenyl] pentyl acetate (VCC904125))

In silico calculation

All computational procedures were performed using the Schrödinger software suite (Release 2019-2, Schrödinger, LLC, New York, NY, USA). Three-dimensional structures of the compounds were generated with LigPrep employing the OPLS3e force field. Physicochemical properties, including the octanol–water partition coefficient, BBB permeability, and polar surface area, were calculated using QikProp. Unionized, salt-free molecular forms were used as input for all calculations. The molecular surface and electrostatic potential map of VCC904125 were generated based on electron density and ESP data calculated with Jaguar.

Radioligand binding assay

Binding assays were performed by Eurofins Panlabs Discovery Services Ltd. (New Taipei City, Taiwan) using human Jurkat cells. S1R binding was assessed by incubating membrane preparations with the selective antagonist [^{3}H]-haloperidol (8.0 nM) in the presence of a competing concentration of VCC904125 (10 µM). Additional assays were performed to evaluate the binding of VCC904125 to the human Ether-à-go-go-Related Gene (hERG) channel**.**

Reversed-Phase High-Performance Liquid Chromatography (RP-HPLC)

C57BL/6J mice were treated ip. as follows: (i) 20 mg x bwkg-1 VCC904125 and (ii) 20 mg x bwkg-1 FLU. Thirty minutes post-treatment, animals were anesthetized and euthanized by exsanguination. Brain and kidney samples were collected, homogenized, and snap-frozen in liquid nitrogen. Next, samples were resuspended in 1.5 ml milliQ water and 10% NH 4 OH was added, and the mixture was extracted with 2x2 ml EtOAc. The collected organic layers were evaporated, redissolved in 90% MeCN-10% milliQ water 0.1% HCOOH and injected to RP-HPLC. Absorbance under the curve was measured at 254 nm.

In vitro models

Cell culture

Human proximal tubular epithelial cells (HK-2; LGC Standards, cat. no. CRL-2190, American Type Culture Collection, Manassas, VA, USA were cultured in Dulbecco's modified Eagle's medium (DMEM; Gibco, Thermo Fisher Scientific, Waltham, MA, USA) supplemented with 10% fetal bovine serum (FBS; Gibco) and 1% penicillin/streptomycin. The cells were incubated at 37°C in 5% CO_2 and 95% air. For reverse transcription-quantitative polymerase chain reaction (RT-qPCR), the cells were plated at 105 cells/well and subjected to a 24 h serum-free period before treatment. Untreated cells were used as controls.

Hypoxic and inflammatory model

In the hypoxia model, after 24 h of pretreatment with VCC904125 or vehicle, HK-2 cells were placed in a bold line stage top CO_2/O_2 incubator (Okolab, Ottaviano, Italy). which was flushed with a gas mixture of 1% O_2, 5% CO_2, and 94% N_2, and then incubated for 2 h at 37 °C. In the inflammatory model, cells were incubated for 24 hours with 1 µg/mL of lipopolysaccharide (LPS), either alone or in combination with 10 µM VCC904125.

Cell proliferation and lactate dehydrogenase assay

HK-2 cells were treated with VCC904125 at concentrations ranging from 0.001 to 50 µM. Cell viability was assessed using a methyl-thiazole tetrazolium (MTT) assay (M6494, Invitrogen, Carlsbad, CA, USA) according to the manufacturer's instructions. Cytotoxicity was evaluated by measuring lactate dehydrogenase (LDH) release in cell culture supernatants using an LDH assay kit (C20300, Invitrogen) following the manufacturer's protocol.

Real-time quantitative PCR

Total RNA was extracted from the kidney samples using RNeasy RNA Isolation Kit (Qiagen, Germantown, MD). The quantity and quality of isolated RNA was measured on a Nanodrop One (Thermo Scientific, Waltham, MA, USA) device. Real-time RT-qPCR was conducted on a LightCycler 96 system (Roche Diagnostics, Mannheim, Germany), utilizing 1 µL of cDNA per sample, 10 µL of SYBR Green I Master Mix

(Roche Diagnostics, Mannheim, Germany), and 10 pmol μL^{-1} of each specific primer (IDT, Coralville, IA, USA) (**Table 2**). Results were analyzed and normalized to the expression of the *Rn18s* housekeeping gene.

Table 2. Primer sequences for real-time quantitative PCR. *bp* – base pair

Gene name	Regular name	Primer sequence	Product length (bp)	Annealing temperature (°C)
Rn18s	Mouse ribosomal 18S ribosomal RNA	Forward: 5' ACTTAAAGGAATTGACGGAAGGG 3'	183	60
		Reverse: 5' GAATTAACCAGACAAATCGCTCC 3'		
	Rat 18S ribosomal RNA	Forward: 5′ GCGGTCGGCGTCCCCCAACTTCTT 3′	105	60
		Reverse: 5′ GCGCGTGCAGCCCCGGACATCTA 3′		
	Human 18S ribosomal RNA	Forward: 5' GGCGGCGACGACCCATTC 3'	136	60
		Forward: 5' TGGATGTGGTAGCCGTTTCTCAGG 3'		
Havcr1	Mouse Kim-1	Forward: 5' GGTCTCCTTCACAGCAGATG 3'	90	57
		Reverse: 5' CTGATTCATGGTACTGACCTAGA 3'		
	Rat Kim-1	Forward: 5' CGCAGAGAAACCCGACTAAG 3'	194	60
		Reverse: 5' CAAAGCTCAGAGAGCCCATC 3'		
Lcn2	Mouse Ngal	Forward: 5' TGACAACTGAATGGGTGGTG 3'	146	57
		Reverse: 5' GATGCTCCTTGGTATGGTGG 3'		
	Rat Ngal	Forward: 5′ CAAGTGGCCGACACTGACTA 3′	194	57
		Reverse : 5′ GGTGGGAACAGAGAAAACGA 3′		
Il1b	Mouse IL- 1β	Forward: 5' TGCCACCTTTTGACAGTGAT 3'	180	60
		Reverse: 5' CCACAGCCACAATGAGTGAT 3'		
	Human IL- 1β	Forward: 5' CCAATCTTCATTGCTCAAGTGTC 3'	88	57
		Reverse: 5' CATTGCCACTGTAATAAGCCATC 3'		
Tnf	Mouse TNF-α	Forward: 5' AGACCCTCACACTCAGATCA 3'	196	60
		Reverse: 5' ACCTGGGAGTAGACAAGGTAC 3'		
	Human TNF-α	Forward: 5' AACGGAGCTGAACAATAGGC 3'	176	60
		Reverse: 5' GGGCGATTACAGACACAACT 3'		
Il10	Mouse IL-10	Forward: 5' ACAACATACTGCTAACCGACTC 3'	277	57
		Reverse: 5' ACACCTTGGTCTTGGAGCTTAT 3'		
Trp53	Mouse P53	Forward: 5' TTCTCCGAAGACTGGATGACTG 3'	91	57
		Reverse: 5' ATAAGCCTGAAAATGTCTCCTGG 3'		
Bax	Mouse Bax	Forward: 5' TTTTGCTACAGGGTTTCATCCA 3'	152	57
		Reverse: 5' CTCCATATTGCTGTCCAGTTCA 3'		
Il1a	Rat Il-1α	Forward: 5′ GGCTGAGAAAGAGGAGTTCG 3′	152	55
		Reverse: 5′ CCACCCATCTGTCTCCTAGA 3′		
IL6	Rat IL- 6	Forward: 5′ GCCACTGCCTTCCCTACTTC 3′	153	55

		Reverse: 5′ GCCATTGCACAACTCTTTTCTC 3′		
Gene name	**Regular name**	**Primer sequence**	**Product length (bp)**	**Annealing temperature (°C)**
IL6	Human IL- 6	Forward: 5' CCACTCACCTCTTCAGAACG 3' Reverse: 5' TTTTCACCAGGCAAGTCTCC 3'	208	55
Hmox-1	Rat HO-1	Forward: 5′ AGACCGCCTTCCTGCTCAACATT 3′ Reverse: 5′ CATTTTCCTCGGGGCGTCTCTG 3′	160	58
Ccl2	Rat MCP-1	Forward: 5′ ATGCAGTTAATGCCCCACTC 3′ Reverse: 5′ TTCCTTATTGGGGTCAGCAC 3′	167	57
HIF1A	Human Hif 1α	Forward: 5' CATAAAGTCTGCAACATGGAAGGT 3' Reverse: 5' ATTTGATGGGTGAGGAATGGGTT 3'	148	58
EPAS 1	Human Hif 2α	Forward: 5' GACAAGGAGAAGAAAAGGAGTA 3' Reverse: 5' GCTCATAGAACACCTCCGTC 3'	100	57
TLR 2	Human TLR 2	Forward: 5'- TCGGAGTTCTCCCAGTTTCT-3' Reverse: 5' GCTTCAACCCACAACTACCA 3'	169	60
TLR 4	Human TLR 4	Forward: 5' CGTGGAGGTGGTTCCTAATA 3' Reverse: 5' GCCTCAGGGGATTAAAGCTC 3'	116	60
NFKB1	Human NF-κB	Forward: 5' GCGGCTCATGTTTACAGCTT 3' Reverse: 5' CGAATCTGGATGTCATCTTTCTG 3'	213	55

Western Blot

All reagents were purchased from Bio-Rad (Hercules, CA, USA), unless stated otherwise. Kidney tissue samples were homogenized in a Cell Extraction Buffer (Invitrogen) with Precellys 24 Evolution (Bertin, Montigny-le-Bretonneux, France), followed by centrifugation. The supernatant containing total protein was collected, and protein concentration was measured via the Lowry assay. Equal amounts of protein (20 µg/sample) were separated on a 4-20% gradient Mini-PROTEAN TGX SDS-polyacrylamide precast gel and transferred to nitrocellulose membranes. Membranes were blocked for 1 h at room temperature () with 5% non-fat dry milk (NFM) or 5% bovine serum albumin (BSA) in Tris-buffered saline. Primary antibodies (p NF-κB (1:1000; ab86299), pCaMkII (1:500; 12716); Cell Signaling Technology, Danvers, MA, USA), Hif1α (1:250; 14179; Cell Signaling Technology), and cCasp3 (1:500; 9661; Cell Signaling Technology, Danvers, MA, USA) (**Table 3**) were incubated with the membranes overnight at 4°C. The membranes were washed in 0,1% TBS-Tween 20,

followed by incubation with the corresponding HRP-conjugated secondary antibodies. Reactive bands were detected using enhanced chemiluminescence and were quantified densitometrically by Image Lab (version 6.1; Bio-Rad Laboratories, Hercules, CA, USA). Results were normalized for Ponceau S staining and intermembrane control.

Table. 3 Primary antibodies list

Antibody	Vendor	Catalogue number	Dilution	Secondary antibody	Secondary antibody dilution	Secondary incubation time
cCasp3	Cell Signaling Technology, Leiden, Netherlands	9661	1:500	Goat anti rabbit	1:2000	1 h
Hif1α	Cell Signaling Technology, Leiden, Netherlands	14179	1:250	Goat anti rabbit	1:2000	1 h
pCaMkII	Cell Signaling Technology, Leiden, Netherlands	12716	1:500	Goat anti rabbit	1:2000	1 h
pNF-κB	Abcam, Cambridge, UK	ab86299	1:1000	Goat anti rabbit	1:3000	1 h

Histology

Kidney tissue samples were fixed in 4% buffered paraformaldehyde (pH 7.4), embedded in paraffin, and sectioned at a thickness of 3 μm. Sections were stained with periodic acid-Schiff (PAS) to assess tubular injury.

To evaluate structural injury in the IR model, a semi-quantitative analysis was performed on eight regions of interest (ROI) per kidney section. Tubular damage scores were calculated based on the severity and extent of morphological alterations, as outlined in (**Table 4)**. The average score for each sample was determined using the formula, where *i* denotes the ROI and *j* indicates the damage grade.

$$\frac{\sum_{i=1}^{8}\sum_{j=1}^{4} Area_j * Grade}{8}$$

Table 4. Scoring system used for tubular injury evaluation

Grade		Area	
0	Healthy	0	0 %
1	Brush border thinning + vacuolization	1	1-5 %
2	Moderate brush border damage + distal tubular dilation	2	5-25 %
3	Brush border loss + onset of necrosis	3	25-50 %
4	Tubular necrosis	4	50-75 %
		5	75-100 %

In the ATx and CI models, renal structural injury was assessed by quantification of tubular dilatation (loss of tubular cell mass, epithelial flattening, loss or thinning of brush border). Tubular luminal areas were measured across five ROIs/kidney (200× magnification), selected with Panoramic Viewer software (software version 1.15.4., 3DHISTECH, Budapest, Hungary). Tubular lumens were digitally highlighted in black, and their pixel counts were measured and averaged for each kidney using Adobe Photoshop CS6 (San José, California, USA) and ImageJ (U. S. National Institutes of Health, Bethesda, Maryland, USA).

Apoptosis detection by Terminal deoxynucleotidyl transferase dUTP nick end labeling (TUNEL) assay

5-µm-thick rat kidney tissue sections were mounted on Superfrost slides (Thermo Shandon, Runcorn, UK) and then manually deparaffinized. Labeling of apoptotic cells was performed using the TUNEL assay with the Apoptag Peroxidase *In Situ* Apoptosis Detection Kit (Millipore, Billerica, MA, USA). Sections were permeabilized with proteinase K for 15 min at RT, then washed before blocking endogenous peroxidase activity with 3% H_2O_2:methanol mixture. Following permeabilization, slides were incubated with the TUNEL reaction mixture, containing 30% terminal deoxynucleotidyl transferase (TdT) enzyme for 1 h at RT, after which a stop buffer was added. Slides were incubated with anti-Dioxigenin Conjugate for 30 min at RT. The color reaction was catalyzed using DAB peroxidase substrate. TUNEL-positive cells were counted in five ROIs of ×200 magnification per kidney. The analysis was performed using Adobe Photoshop CS6 (Adobe Inc., San Jose, CA, USA) and Image J (software version 1.54a, National Institute of Health, Bethesda, MD, USA) softwares.

Immunohistochemistry for CD45, CD68 and CD4 detection

Sections (1 µm thick) were manually deparaffinized and rehydrated through a series of graded alcohols. Endogenous peroxidase activity was blocked by incubating the slides in a 3% hydrogen peroxide solution mixed with methanol for 20 min at RT. Antigen retrieval was performed by immersing the slides in 0.05 mM citrate buffer (pH 6.0) and heating them to 93 °C for 10 min. After cooling, the sections were incubated overnight at 4 °C with a primary anti-CD45 (1:100, Abcam, ab10558, Cambridge, UK), anti-CD68 ((1:100, Abcam, ab125212, Cambridge, UK), and anti-CD4 (1:100, Abcam, ab183685, Cambridge, UK) antibodies diluted in phosphate-buffered saline (PBS). The following day, sections were rinsed and incubated with a biotinylated secondary antibody (DakoCytomation, Glostrup, Denmark) for 15 min at RT. Visualization of antibody binding was achieved using the avidin-biotin-peroxidase complex (ABC) method (Dako) and aminoethyl carbazole as the chromogen. Quantification of interstitial leukocyte infiltration was conducted on entire kidney sections using Qpath software (version 0.1.2, Queen's University, Belfast, UK).

Statistical analysis

Data are presented as means ± SDs. Statistical analyses were carried out using Prism software (version 10.6.1; GraphPad Software, La Jolla, CA). Grubbs's test was used to identify outliers. The Shapiro-Wilk test was applied to assess the normality of data distribution. For multiple comparisons and assessment of potential interactions, one-way ANOVA was performed, followed by Holm-Sidak post hoc analysis. In cases where the data did not follow a normal distribution, the Kruskal-Wallis ANOVA on ranks was used. *p*-values of less than 0.05 were considered statistically significant.

4. Results

4.1. S1R agonist FLU improves graft function and attenuates tubular injury after transplantation

Based on our previous results demonstrating renoprotective effects of FLU in a rat IRI model, we evaluated whether S1R activation is protective in the setting of whole-kidney transplantation. To investigate this, a rat model comprising of 2 h of CI followed by kidney isograft autotransplantation was performed.

Twenty-four hours after reperfusion following renal transplantation, renal functional parameters, BUN, aspartate transaminase (AST), and serum creatinine were elevated, suggesting the development of ischemia-induced AKI. FLU supplementation to the preservation solution ameliorated serum creatinine and AST levels, indicating milder injury (**Figure 8a-c**).

Measuring mRNA expression levels of kidney injury molecule-1 (Kim-1; *Havcr1*) and neutrophil gelatinase-associated lipocalin (Ngal; *Lcn2*) is crucial for early detection and monitoring of kidney injury **(Figure 8d-e)**. Both tubular injury marker levels were significantly reduced in kidneys preserved with FLU-supplemented solution 24 hours after ATx.

Heme oxygenase-1 (HO-1; *Hmox1*) is upregulated during AKI and has been proposed as a potential biomarker for early detection and assessment of renal tubular injury and repair processes **(Figure 8f)**. Following ATx, a significant elevation in *Hmox1* mRNA expression was observed, which was reduced by S1R agonist FLU.

Histological changes were evaluated in PAS-stained kidney tissue sections by measuring tubular lumen areas (**Figure 8g-h)**. Twenty-four hours after ATx, kidneys stored in a preservation solution supplemented with FLU (ATxFLU) exhibited only moderate tubular damage, necrosis, and brush border loss compared to the untreated ATx group, as shown by the diminished tubular lumen area increment.

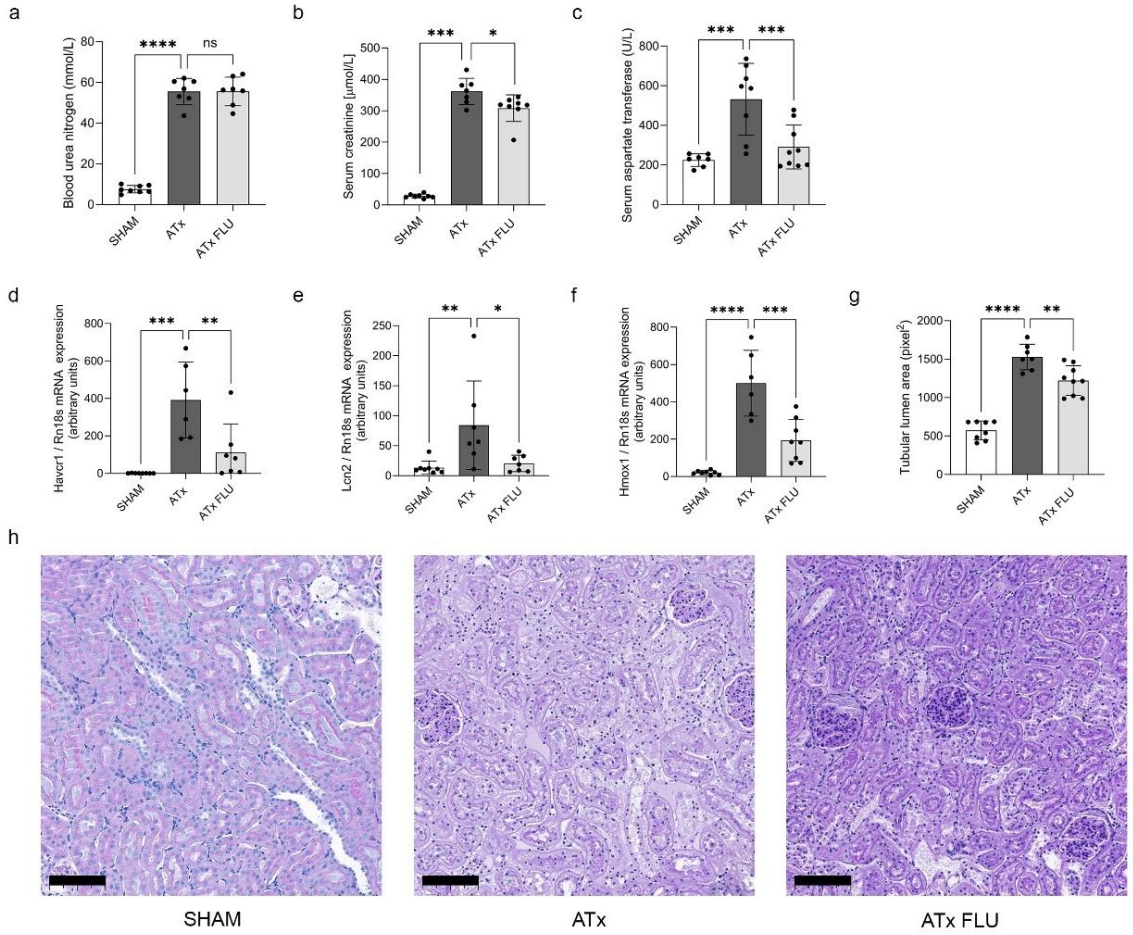

Figure 8. Sigma-1 receptor agonist fluvoxamine (FLU) protects against transplant injury. Renal functional parameters **(a)** blood urea nitrogen (BUN), (**b**) serum creatinine, and **(c)** serum aspartate transferase (AST). mRNA expression levels of **(d)** kidney injury molecule 1 (Kim-1; *Havcr1*), **(e)** neutrophil gelatinase-associated lipocalin (NGAL; *Lcn2*), and **(f)** heme oxygenase 1 (*Hmox1*) genes. **(g)** Mean area of proximal tubular lumen (pixel). **(h)** Representative images of periodic acid-Schiff-stained rat kidney sections (scale bar = 100 µm). *p<0.05; **p<0.01; ***p<0.001; ****p<0.0001, ns. = not significant, n = 6–8/group.

4.2. FLU reduces inflammation after kidney transplant

Inflammation after transplantation plays a crucial role in kidney allograft loss. To assess whether S1R activation can mitigate inflammation after transplantation, we performed anti-CD45 immunohistochemistry and measured mRNA expression of monocyte chemoattractant protein 1 (MCP-1; *CCL2*), *IL1A*, and *IL6 (***Figure 9a-c)**. Anti-CD45 staining revealed a massive decrement in leukocyte infiltration in kidneys stored in a preservation solution containing FLU (**Figure 9d-e**). In parallel, *MCP-1*, *IL1A*, and *IL6* mRNA expressions were decreased in kidneys stored with FLU.

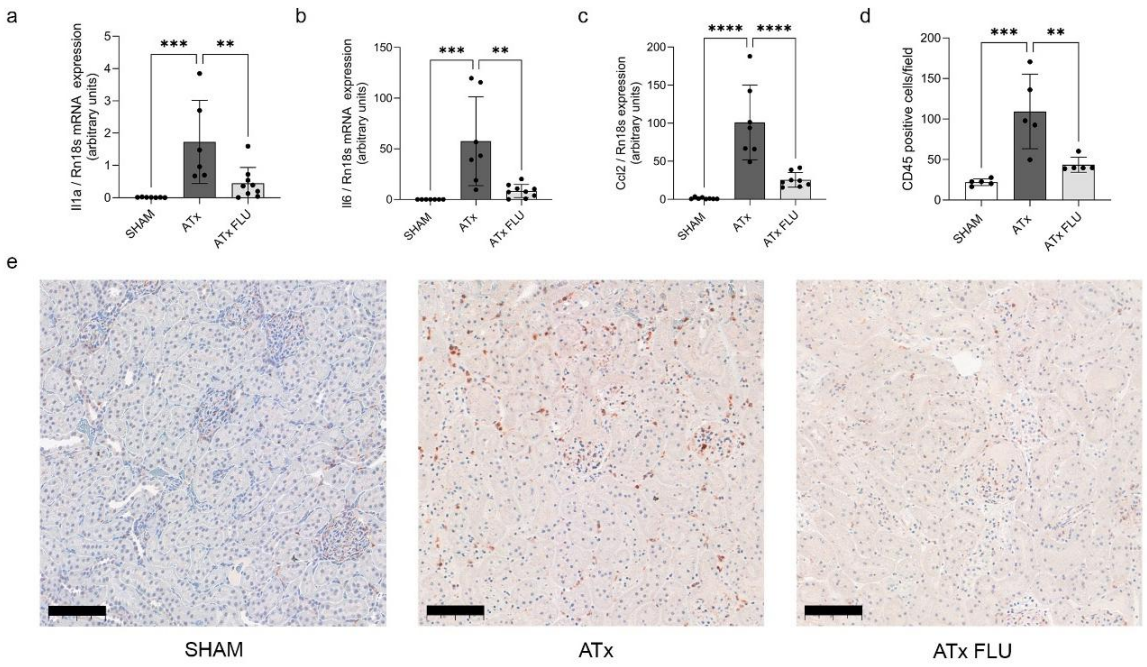

Figure 9. S1R agonist FLU protects against post-transplant inflammation. mRNA expression levels of **(a)** interleukin 1 alpha (*Il1a*), **(b)** interleukin 6 (*Il6*), and **(c)** monocyte chemoattractant protein 1 (*Ccl2*). **(d)** Mean number of CD45-positive cells/field of view. **(e)** Representative images of anti-CD45 labeled rat kidney sections (scale bar = 100 µm) *p<0.05; **p<0.01; ***p<0.001; ****p<0.0001, n = 6–8/group.

4.3. Addition of FLU to preservation solution improves renal integrity during cold storage

To simulate the hypothermic preservation phase before deceased donor kidney transplantation, kidneys were flushed and perfused with preservation solution and stored under ice-cold conditions for various time periods, mimicking the physiological and biochemical stresses of clinical cold storage

Structural injury was already visible after 2 h of cold storage. Supplementation of the preservation solution with FLU mitigated the progression of injury so profoundly that the degree of cold–storage–induced renal damage observed after 24 h with FLU was comparable to that detected after 2 h without FLU (**Figure 10**).

The anti-apoptotic effect of FLU was confirmed by TUNEL assay and Caspase-3 immunostaining, which both showed a reduced number of positive cells after both 2 and 24 h of cold storage (**Figure 11-12)**.

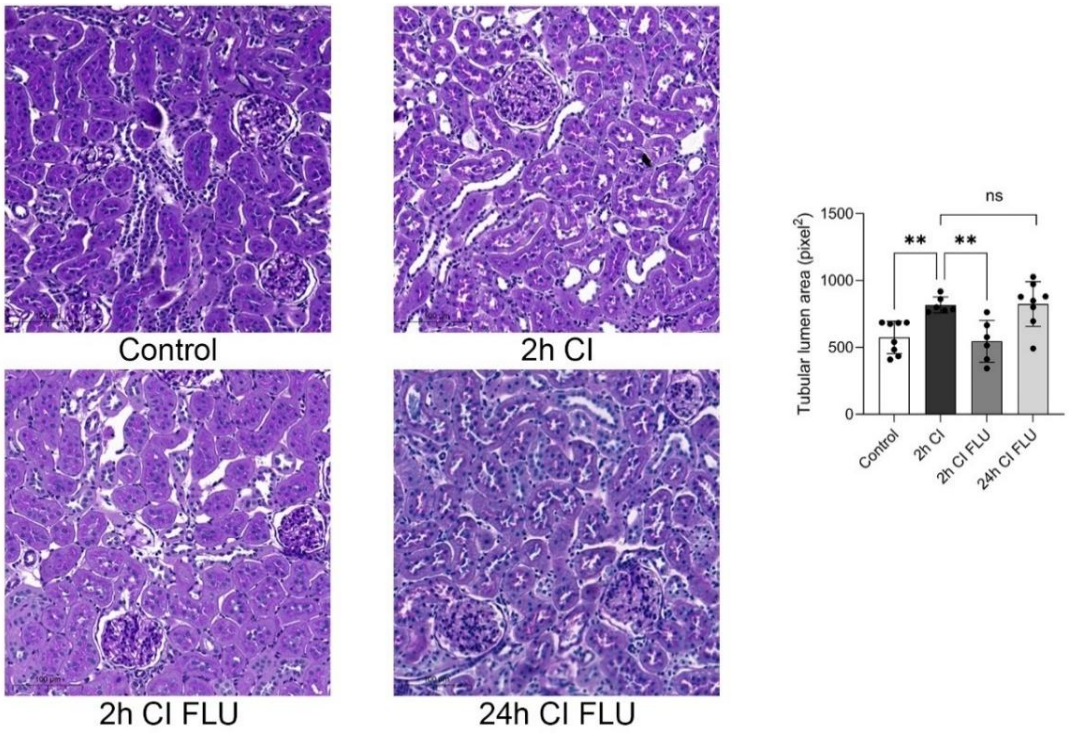

Figure 10. FLU Supplementation improves renal structural damage. Mean area of proximal tubular lumen (pixel) evaluated on periodic acid-Schiff-stained rat kidney sections (scale bar = 100 µm).;**p<0.01; ns. = not significant, n = 6–8/group.

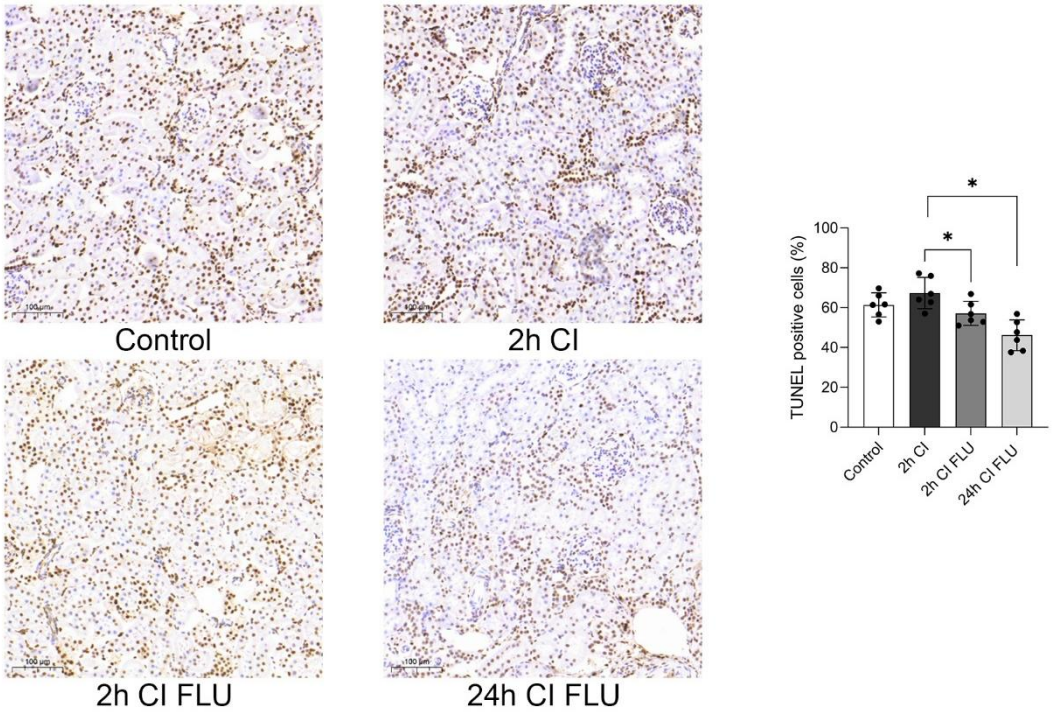

Figure 11. FLU Supplementation reduces renal apoptosis. Mean number of apoptotic cells evaluated on rat kidney sections labeled with TUNEL assay. (scale bar = 100 µm). *p<0.05; n = 6–8/group.

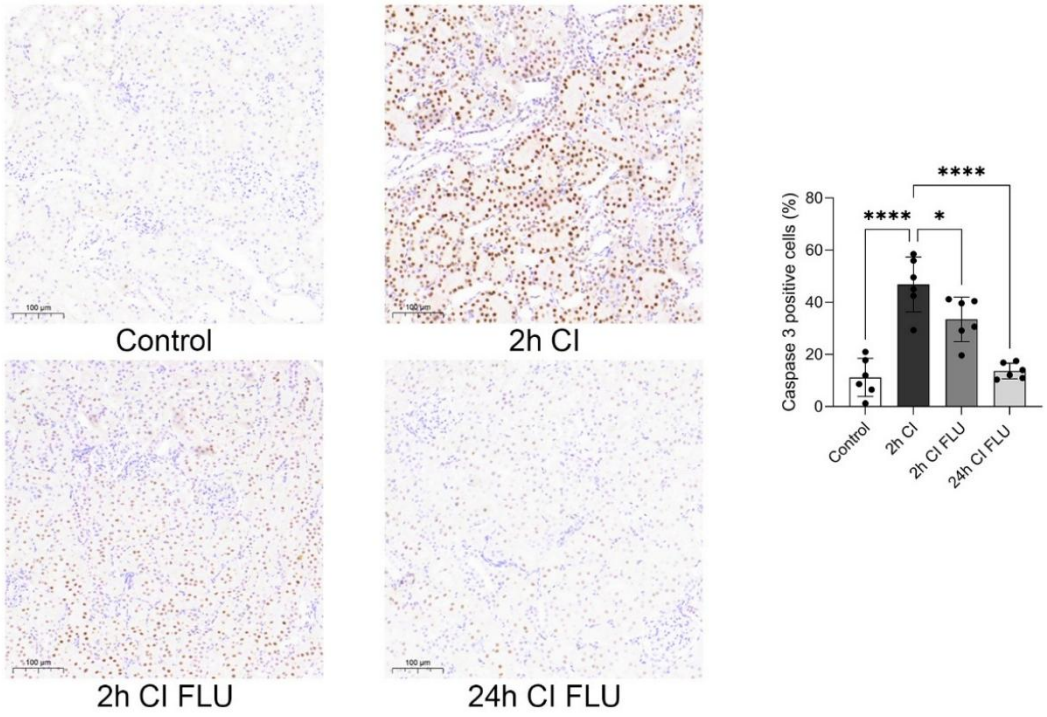

Figure 12. FLU Supplementation mitigates renal apoptosis after cold ischemia. Mean number of Caspase-3 positive cells/field of view evaluated on anti-Caspase-3 labeled rat kidney tissue sections (scale bar = 100 µm). *p<0.05; ****p<0.0001, n = 6–8/group.

4.4. The protective effects of FLU are nullified in S1R knockout ($S1R^{-/-}$) mice

To confirm that the renoprotective effects of FLU were directly mediated by S1R, the CI model was repeated in $S1R^{+/+}$ and $S1R^{-/-}$ mice. In $S1R^{+/+}$ mice, administration of FLU significantly mitigated tubular structural alterations and decreased the extent of apoptosis following 24 h of CI, while these effects were not observed in $S1R^{-/-}$ mice (**Figure 13-14**).

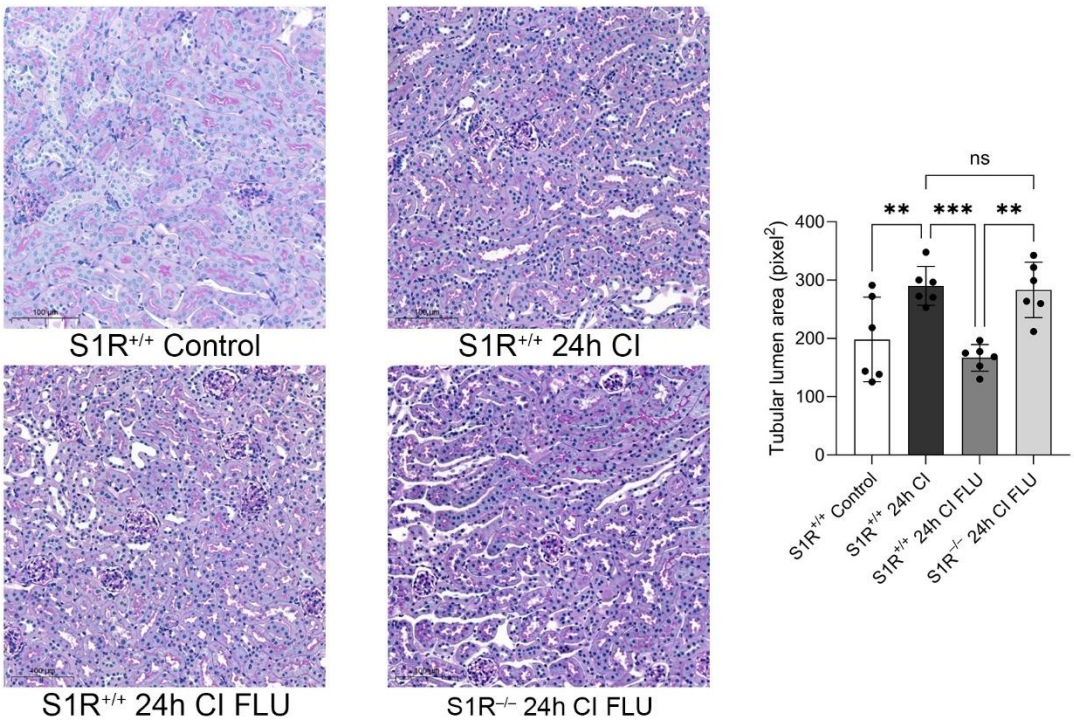

Figure 14. Improved renal preservation with FLU during cold storage is observed in $S1R^{+/+}$ but absent in $S1R^{-/-}$ mice. Mean area of proximal tubular lumen (pixel) evaluated on periodic acid-Schiff-stained mouse kidney sections. = 100 µm). **p<0.01; ***p<0.001; ns. = not significant, n = 5–6/group.

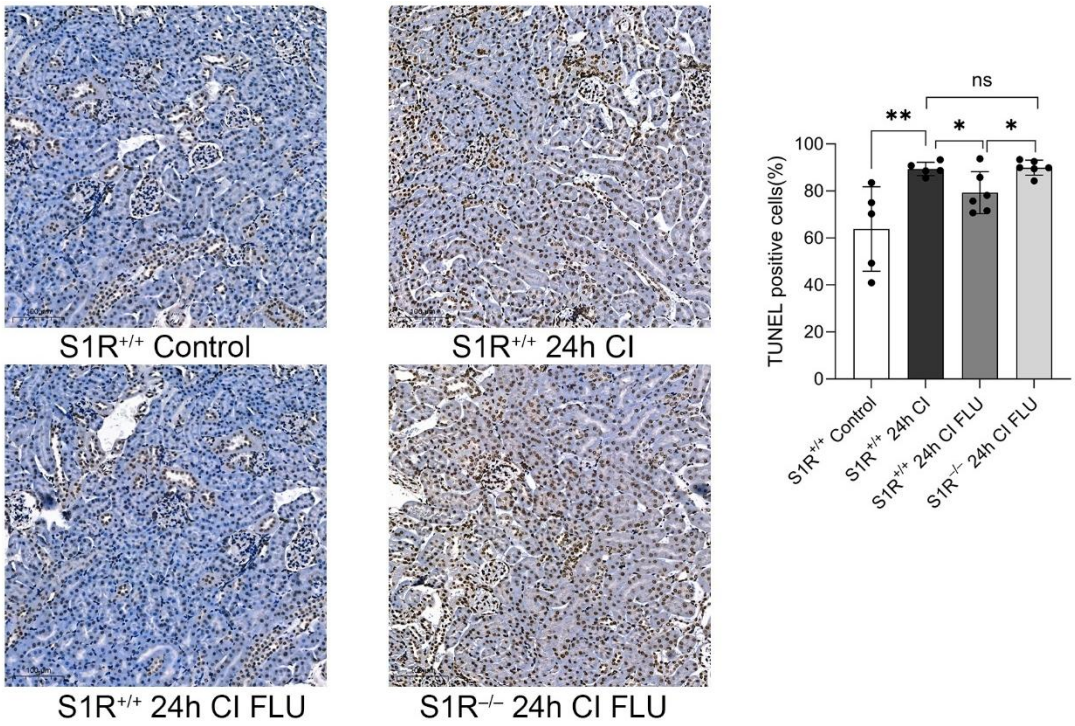

Figure 14. Decreased apoptosis with FLU during cold storage is observed in S1R$^{+/+}$ but absent in S1R$^{-/-}$ mice. Mean number of apoptotic cells evaluated on mouse kidney sections labeled with TUNEL assay (scale bar = 100 µm). *p<0.05; **p<0.01; ns. = not significant, n = 5–6/group.

4.5. Characterization of VCC904125: Blood–Brain Barrier Penetration, Binding Affinity, and Cellular Effects

Based on the high BBB permeability of FLU, novel S1R agonists with limited BBB penetration were developed and tested in the following experiments.

In silico pharmacokinetic predictions were conducted to assess the BBB permeability (QPlogBB) and lipophilicity (QPlogPo/w) of the compounds. As expected, FLU showed a strong ability to cross the BBB, whereas VCC904125 exhibited high QPlogPo/w values—reflecting its chemical structure—which are consistent with limited BBB penetration. Polar surface area (PSA), a key factor of a molecule's ability to cross the BBB, was also calculated. VCC904125 showed the highest PSA value of 83.5 $Å^2$ and indicating that this compound is expected to display minimal CNS penetration (**Figure 15a**).

The competitive radioligand binding assay was performed to demonstrate that VCC904125 binds to S1R. The assay showed that VCC904125 induced a maximal displacement similar to that of FLU at 10 µM, coupled with low hERG affinity (**Figure 15b**).

To assess the effect of VCC904125 on renal cell proliferation and cytotoxicity, MTT and LDH assays were performed. The MTT assay showed no significant changes in cell proliferation at any of the tested concentrations, indicating that VCC904125 does not impair cell viability after 24 h of exposure. In contrast, the two highest concentrations (25 and 50 µM) elicited a significant increase in LDH release; therefore, the 10 µM concentration was selected for future experiments (**Figure 15c-d**).

a

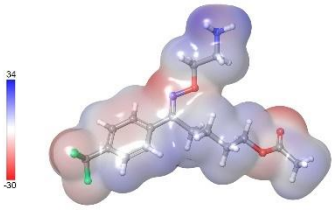

b

Name	QPlogPo/w	QPlogBB	PSA	hERG (% Inh)	Sigma σ1 (% Inh)
Fluvoxamine unionized	3,108	0,01	54,21 A^2	21	95
VCC904125 unionized	3,078	-0,79	83,54 A^2	27	89
VCC553789 unionized	2,227	-0,72	57,71 A^2	-9	9
VCC846743 unionized	4,062	-0,49	63,24 A^2	16	9

c

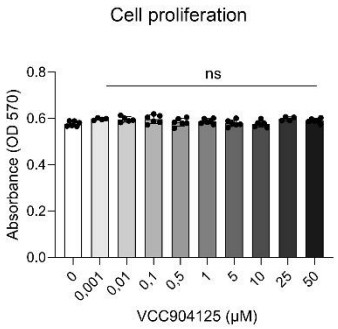

d

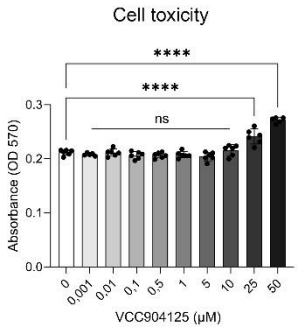

Figure 15. Physicochemical and cellular characterization of VCC904125. (a) Electrostatic potential surface of VCC904125 (kcal/mol). **(b)** *In silico* calculated partition coefficient (QPlogPo/w), brain-to-blood distribution ratio (QPlogBB), and polar surface area, along with inhibition values (%) from the radioligand binding assay. **(c)** Cell proliferation and **(d)** cellular toxicity were assessed 24 hours after treatment with different concentrations of VCC904125 (VCC) using MTT and LDH assays, respectively. (****p<0.001; ns. = not significant, n=5-6/group)

4.6. Sigma-1 Receptor Agonist VCC904125 Does Not Cross the BBB

To verify the limited ability of VCC904125 to cross the BBB, RP-HPLC analysis was performed using both FLU and VCC904125 in kidney and brain tissue homogenates. As expected, both compounds were detected in kidney samples; on the other hand, only FLU was detected in brain homogenates, while VCC904125 remained below the detection threshold (**Figure 16a-b**). These findings provide experimental confirmation of the compound's restricted BBB permeability, consistent with its physicochemical properties and *in silico* predictions.

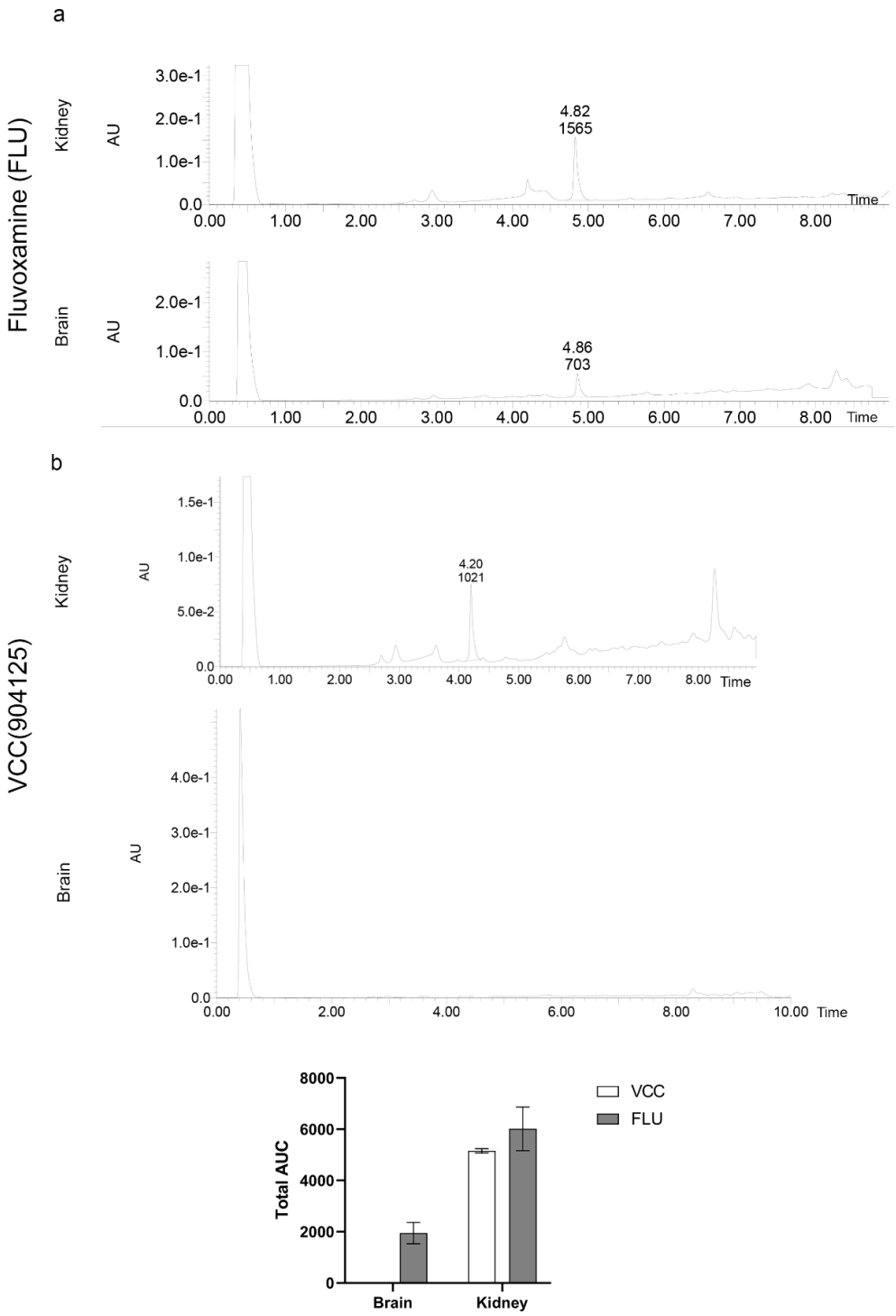

Figure 16. Sigma-1 Agonist VCC904125 Does Not Cross the Blood–Brain Barrier. Representative images of RP-HPLC chromatograms of **(a)** kidney and brain samples of mice treated with fluvoxamine; **(b)** kidney and brain samples of mice treated with VCC904125. (AUC = Absorbance under the curve)

4.7. VCC904125 mitigates tubular hypoxia and LPS-induced inflammation in HK-2 cells

To evaluate the effects of VCC904125 under hypoxic conditions, HK-2 cells were exposed to 1% O_2 for 2 h to simulate ischemia/reperfusion-induced hypoxia. HIF proteins, particularly *HIF1A* a play a pivotal role in the cellular adaptation to oxygen deprivation. Here, under hypoxic conditions, HK-2 cells showed significant activation of the hypoxia response pathway. S1R agonist VCC904125 treatment decreased *HIF1A* mRNA expression elevation, suggesting reduced cellular hypoxic stress (**Figure 17a-b**).

Inflammation plays a pivotal role in IRI. The interconnected pathways of TLRs, NF-κB, and interleukins are central components of the inflammatory response after IRI. To investigate whether S1R activation can attenuate inflammation in proximal tubular cells, we analyzed the mRNA expression of *TLR2*, *TLR4*, *NFKB1*, *IL1B*, *IL6*, and *TNF* after LPS induction in HK-2 cells. LPS increased TLR2 and TLR4 expression, leading to a subsequent rise in NFKB1 and proinflammatory cytokine expression. VCC904125 treatment reduced the expression of all measured markers (**Figure 17c-h**).

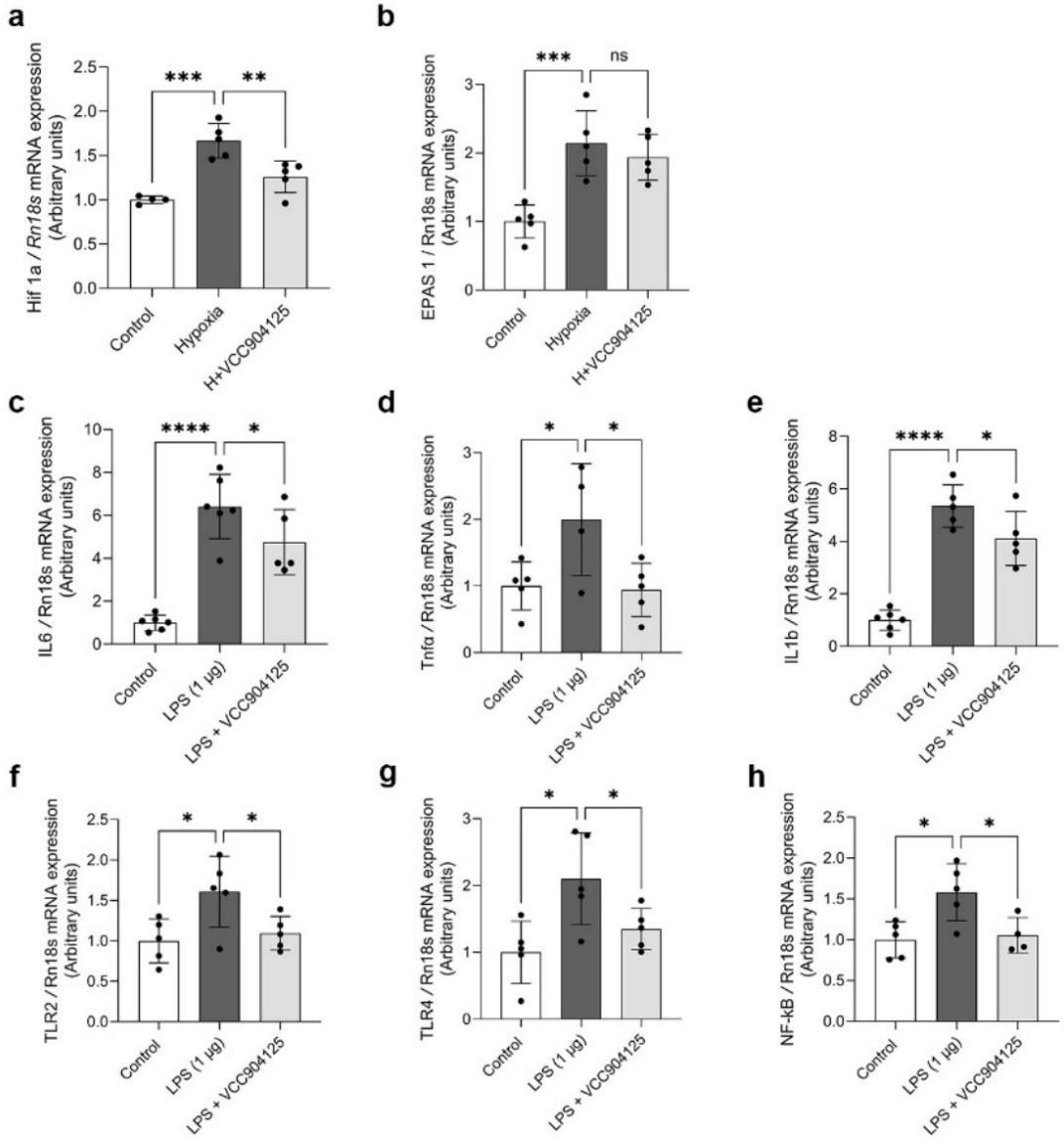

Figure 17. Sigma-1 receptor agonist VCC 904125 reduced LPS-induced inflammation and ameliorated the cellular response to tubular hypoxia and abolished the activation of the HIF-1α pathway. (**a-h**) mRNA expression of hypoxia-inducible factor-1α (*HIF1A*), hypoxia-inducible factor-2α (*EPAS1*), interleukin-6 (*IL6*), tumor necrosis factor-α (*TNF*), interleukin-1β (*IL1B*), toll-like receptor-2 (*TLR2*), toll-like receptor-4 (*TLR4*) and nuclear factor κB (*NFKB1*). *p<0.05; **p<0.01; ***p<0.001; ****p<0.000, ns. = not significant, n=4-5/group.

4.8. VCC904125 ameliorates renal ischemic injury 24h after reperfusion

To evaluate the renoprotective effect of VCC904125, mice were treated with the compound 30 min before the ischemic insult. Renal function was substantially impaired 24 h after reperfusion, as evidenced by significantly elevated BUN and serum creatinine levels. S1R agonist VCC904125 treatment reduced BUN levels, indicating more preserved renal function (**Figure 18a-b**).

Highly specific and sensitive makers of tubular injury, KIM-1 and NGAL, were measured to assess the extent of renal damage. IRI led to a marked increase in mRNA expression of both markers, reflecting severe tubular injury. Treatment with VCC904125 reduced KIM-1 and NGAL expressions, indicating significant protection against tubular injury (**Figure 18c-d**).

Histological injury was assessed on PAS-stained kidney sections, demonstrating pronounced hyaline accumulation, vacuolization, loss of brush border, and tubular necrosis after IRI, indicating severe structural damage. VCC904125 mitigated the extent of acute tubular necrosis (**Figure 18e**).

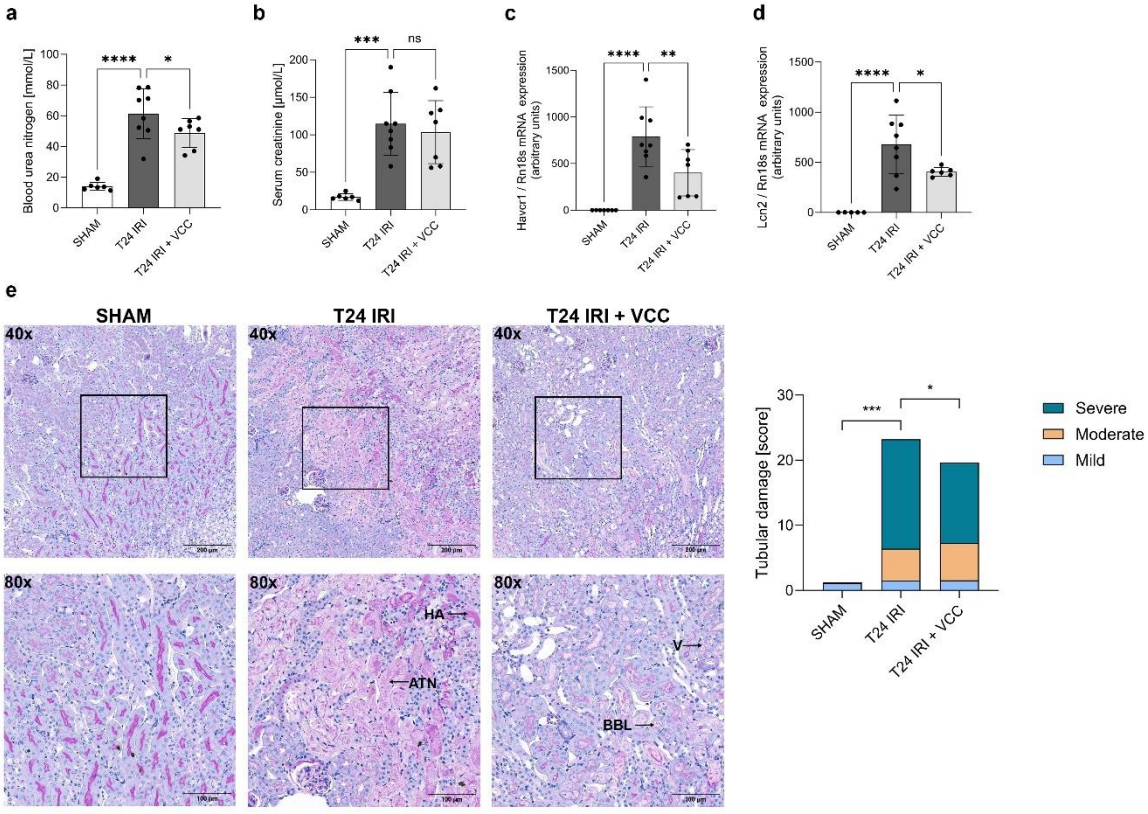

Figure 18. VCC904125 (VCC) ameliorates renal ischemic injury. Renal functional parameters **(a)** blood urea nitrogen (BUN) and **(b)** serum creatinine. mRNA expression levels of **(c)** kidney injury molecule 1 (KIM-1; *Havcr1*) and **(d)** neutrophil gelatinase-associated lipocalin (NGAL; *Lcn2*). Representative images of periodic acid-Schiff-stained kidney tissue sections to evaluate **(e)** renal IRI (scale bar = 200 µm and 100 µm; magnification:40x and 80x; ATN: acute tubular necrosis, HA: Hyalin accumulation, BBL: Brush border loss, V: vacuolization). *p<0.05; **p<0.01; ***p<0.001; ****p<0.0001, n=6-8/group.

4.9. The beneficial effects of VCC904125 are diminished in S1R$^{-/-}$ mice

To confirm that the renoprotective mechanisms of VCC904125 are mediated by S1R, the renal IRI model was repeated on S1R$^{-/-}$ mice. Neither renal functional parameters nor tubular injury markers nor PAS-stained histological assessments indicated any renoprotective effect of S1R agonist VCC904125 in S1R$^{-/-}$ mice (**Figure 19**).

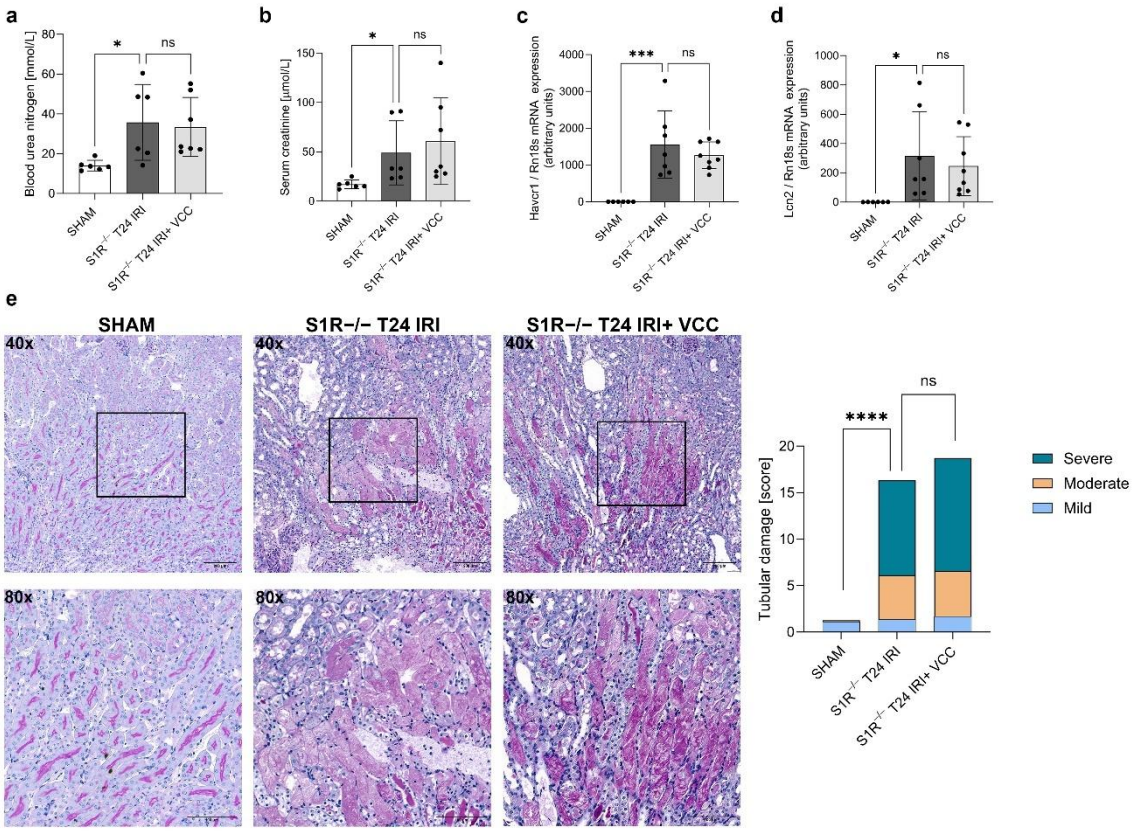

Figure 19. The protective effects of VCC904125 are diminished in S1R$^{-/-}$ mice. Renal functional parameters **(a)** blood urea nitrogen (BUN) and **(b)** serum creatinine. mRNA expression levels of **(c)** kidney injury molecule 1 (KIM-1; *Havcr1*) and **(d)** neutrophil gelatinase-associated lipocalin (NGAL; *Lcn2*). Representative images of periodic acid-Schiff-stained kidney tissue sections to evaluate **(e)** renal IRI (scale bar = 200 µm and 100 µm; magnification:40x and 80x;). *p<0.05; **p<0.01; ***p<0.001; ****p<0.000, ns. = not significant, n=6-8/group.

4.10. Sigma 1 receptor agonist VCC904125 mitigates IRI-induced hypoxia, apoptosis, and reduces inflammation following IRI

Twenty-four hours after IRI, both *HIF1A* and *HIF2A* were elevated, suggesting acute and chronic hypoxia in the T24 IRI group. S1R agonist VCC904125 treatment ameliorated HIF1A protein level and *HIF2A* mRNA expression (**Figure 20a-b**).

Apoptosis during IRI-induced AKI is primarily mediated by the p53–Bax signaling cascade and subsequent caspase-3 activation. mRNA levels of *p53* and *Bax* were upregulated in the IRI group but remained unchanged after VCC904125 treatment. Similarly, the increase in cleaved caspase-3 protein level observed following IRI was significantly reduced in VCC904125-treated mice (**Figure 20c-e**).

The NF-κB pathway is a central regulator of pro-inflammatory gene induction during IRI-induced AKI. To confirm the anti-inflammatory effect of S1R activation, phosphorylated NF-κB and phosphorylated CaMKII protein levels were measured. VCC904125 treatment reduced both protein levels 24h after IRI. In parallel, inflammatory cytokines *IL1B* and *TNF* were also decreased in the T24 IRI+VCC904125 group (**Figure 20f-j**).

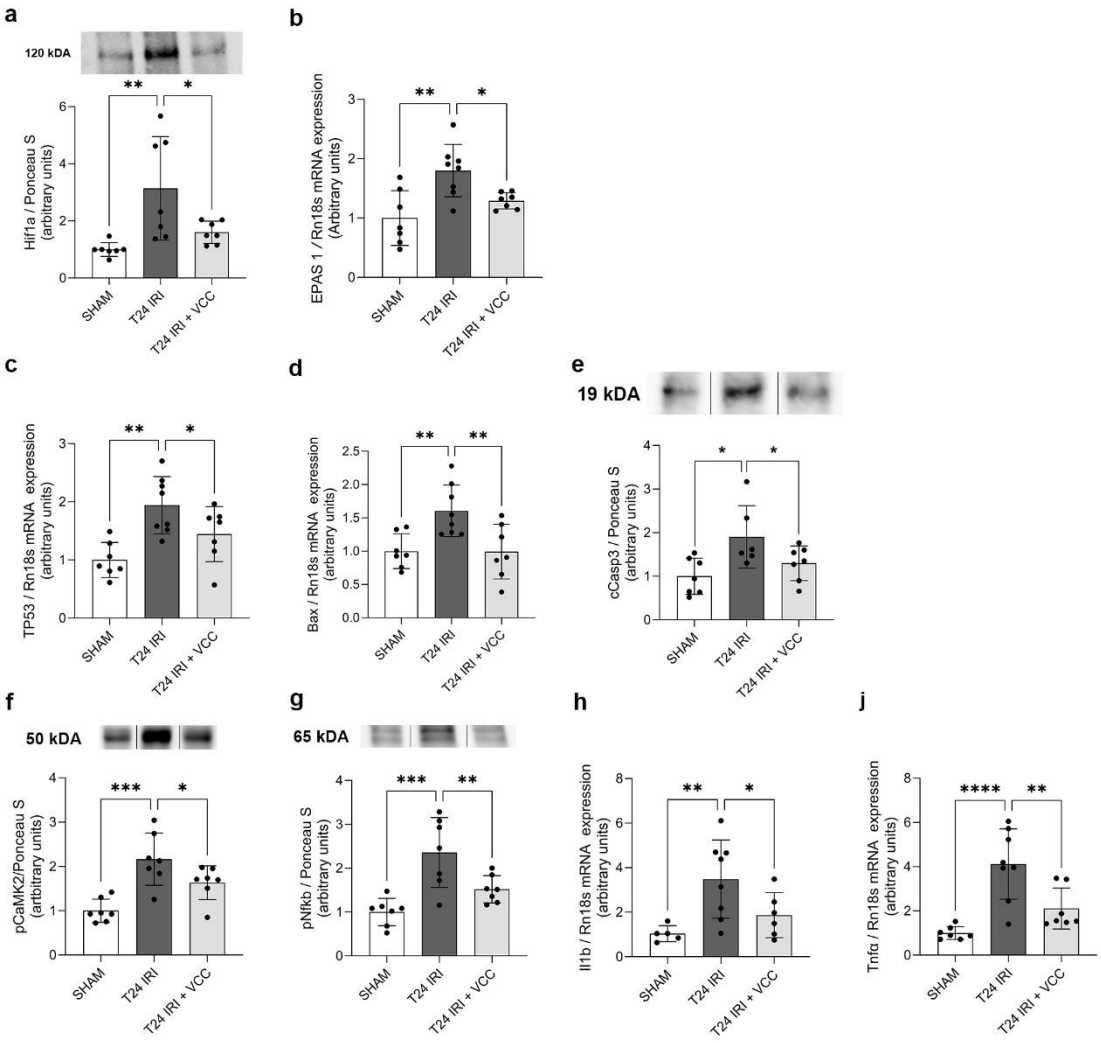

Figure 20. Sigma-1 receptor agonist VCC904125 (VCC) ameliorated hypoxia, diminished apoptosis, and attenuated the inflammatory response 24 hours after ischemia/reperfusion injury (T24 IRI). (a) Protein level of hypoxia-inducible factor-1α (HIF1A). mRNA level of **(b)** hypoxia-inducible factor-2α (*EPAS1*), **(c)** tumor protein P53 (*Trp53*) and **(d)** Bcl2-associated X, apoptosis regulator (*Bax*). Protein level of **(e)** cleaved caspase 3 (cCasp3), **(f)** phosphorylated Ca2+/calmodulin-dependent protein kinase II (pCAMKII) and **(g)** phosphorylated nuclear factor-kappa B (pNF-κB). mRNA expression levels of **(h)** interleukin IL-1β (*Il1b*) and **(j)** Tumor necrosis factor (TNF)-α (*Tnf*). *p<0.05; **p<0.01; ***p<0.001; ****p<0.0001, n=6-8/group.

4.11. No inflammatory cell infiltration was observed 24 h after ischemic insult

To assess inflammatory cell infiltration, kidney tissue sections were immunolabeled for $CD45^+$ for leukocytes, $CD68^+$ for macrophages, and $CD4^+$ for T cells. No lymphocytic or leukocytic infiltration was observed 24 h after reperfusion. Similarly, no evidence of $CD68^+$ macrophage infiltration was observed in any of the experimental groups **(Figure 21**). These results are likely due to the fact that leukocytes and macrophages usually appear 36-48 hours after injury and peak at 3-5 days.

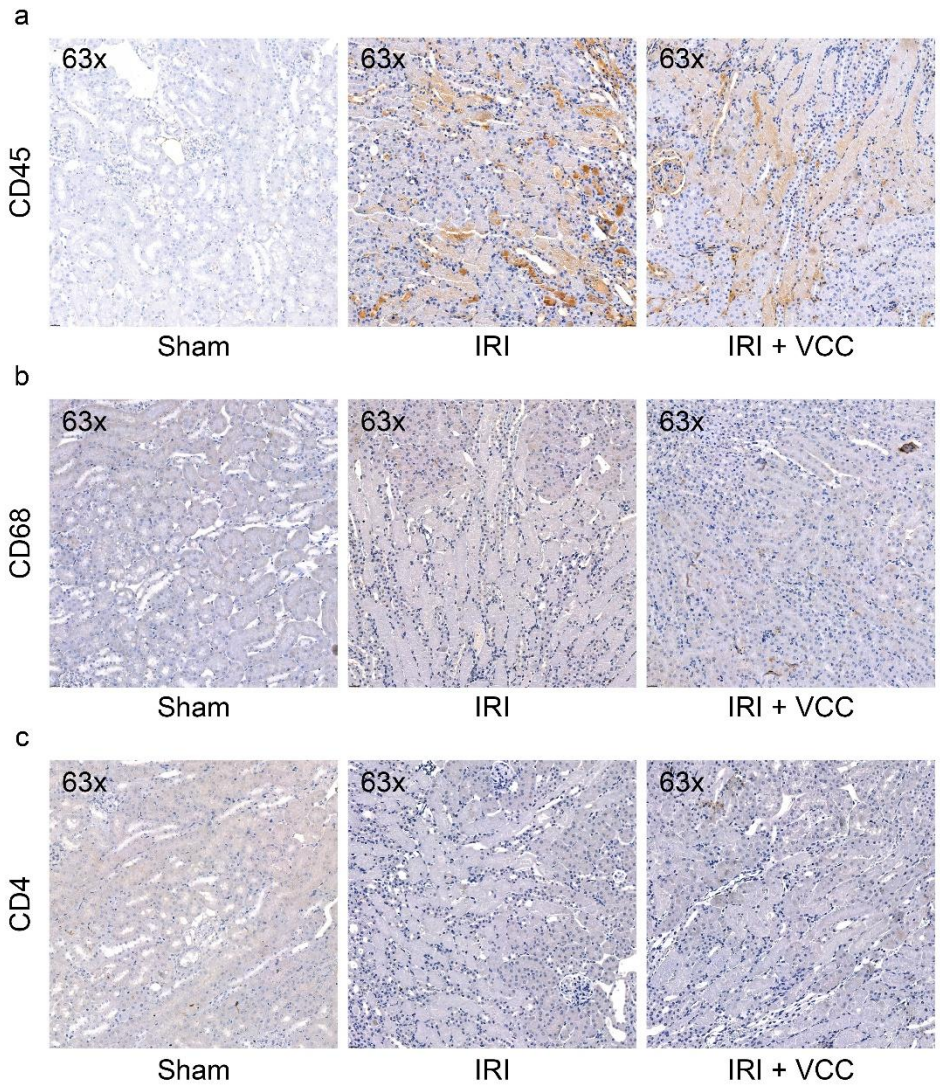

Figure 21. No inflammatory cell infiltration was observed 24 hours after ischemic insult. Representative images of (a) anti-$CD45^+$, (b) anti-$CD68^+$, and c anti-$CD4^+$ labeled kidney sections. Magnification:63x, VCC904125 (VCC), n=6/group.

4.12. S1R agonist VCC904125 ameliorates CI-induced renal injury

To mimic pre-transplant cold storage, kidneys were perfused and maintained in an ice-cold Custodiol HTK preservation solution containing the S1R agonist VCC904125 for 24 h. Tubular dilatation served as an indicator of structural injury in the CI model. In the 24h CI group, extended proximal tubular lumen expansion was observed, indicating loss of tubular cell mass and epithelial flattening. Supplementation with VCC904125 attenuated these morphological changes (**Figure 22**). This suggests that S1R activation alleviates CI-induced tubular damage, potentially improving graft condition before transplantation.

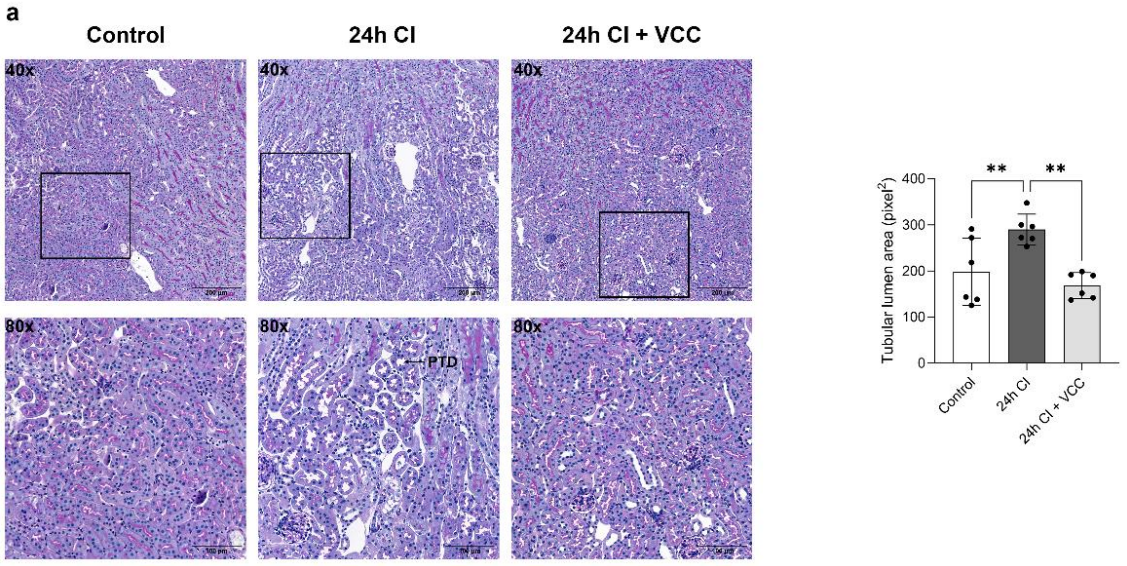

Figure 22. VCC904125 (VCC) mitigates cold ischemic (CI) structural injury. **(a)** Representative images of periodic acid-Schiff-stained kidney tissue sections to evaluate CI injury after 24 hours (scale bar = 200 µm and 100 µm; magnification:40x and 80x; PTD: Proximal tubular dilatation); **p<0.01, n=6/group.

5. Discussion

CKD is a major global health problem, affecting hundreds of millions of people worldwide. It is characterized by the gradual loss of renal function leading to ESRD in many patients, which requires dialysis or RRT. Among current therapeutic options, KTx is considered the gold standard, offering the best long-term outcomes and quality of life. However, transplantation is inevitably associated with IRI, particularly in grafts from cadaver donors, where prolonged CI cannot be avoided. IRI represents a key alloantigen-independent factor for both graft and patient survival, and each hour of CI significantly increases the risk of DGF. In the last decade, several novel surgical techniques and different pharmacological interventions targeting inflammatory pathways and oxidative stress have been developed; no approach has yet produced a substantial clinical breakthrough in mitigating warm IRI–related damage.

S1R is a highly conserved chaperone protein, which has mainly been studied in the CNS, where it modulates key cellular stress responses, including inflammation and hypoxia. As an inter-organelle signaling molecule, S1R is also present in peripheral tissues, where it plays diverse roles in cellular survival (85).

Our group previously described the S1R as a novel mediator of renoprotective mechanisms in various kidney diseases. FLU is a well-known, frequently used SSRI that modulates the serotonergic and noradrenergic systems in the brain. FLU was selected for these experiments because of its high binding affinity for the S1R (Ki = 36 nM) (97,98), in addition to its widespread clinical use and accessibility. We demonstrated the precise renal localization of S1R and, using multiple approaches, showed the renoprotective effect of S1R activation. First, in an *in vivo* rat IRI model, treatment with FLU improved postischemic survival and renal function. These renoprotective effects were mediated through activation of the S1R–AKT–eNOS signaling pathway, resulting in increased NO production. This NO-mediated vasodilation improved post-ischemic renal perfusion, contributing to the overall renoprotective effect (94). Second, we revealed that in females, S1R activation by estrogen enhances the heat shock response in the kidney after an ischemic event, mediating the renoprotection in females compared to males (96). Furthermore, we demonstrated that activation of S1R has protective effects on renal function, inflammation, hypoxia, and fibrosis in diabetic kidney disease (99).

Based on our previous results, we speculated that S1R activation may be protective during a whole-kidney transplantation procedure. To investigate this, we used a rat kidney autotransplantation model with CI, which enabled controlled assessment of ischemic injury in the absence of rejection or confounding effects from immunosuppressive therapy. Deceased donor transplants represent more than 70% of all kidney transplants. To model this clinical scenario and investigate whether S1R activation can mitigate cold ischemic injury, we performed an experimental cold IRI model.

Early post-transplant follow-up is essential for evaluating graft condition and predicting long-term outcomes (100). Zero-time or reperfusion biopsies are usually performed immediately or within the first hours after KTx to assess the extent of IRI and ATN, providing early prognostic information about donor kidney quality, identifying acute injuries and chronic lesions associated with graft survival(101–103). The severity of ATN strongly correlates with poorer outcomes, including DGF and increased graft failure (104). Importantly, recovery of the tubular epithelium after ischemic injury primarily depends on surviving endogenous tubular cells, which dedifferentiate, proliferate, and restore the damaged nephron rather than being replaced by external progenitors (105,106). In parallel to biopsies, early renal functional parameters are measured as a non-invasive indicator of graft recovery. Post-ATx histological changes and renal function were also improved in rats with kidneys perfused with FLU, as evidenced by decreased serum creatinine and tubular injury marker AST levels. In recent years, several papers have reported that traditional renal functional markers are unreliable and have limitations for detecting kidney injury (107,108). Therefore, we measured KIM-1 and NGAL, which are specific and sensitive biomarkers of early tubular damage, and they often reveal kidney injury before more overt clinical signs emerge (109). KIM-1 is expressed by proximal tubular epithelial cells, where its upregulation reflects the extent of structural damage and strongly correlates with the severity of histological injury, while NGAL is mainly produced in the distal nephron and rises rapidly in response to tubular stress, and it has been shown to predict DGF and 1-year graft function (110–112). In our experiment, the RNA expression of both KIM-1 and NGAL was robustly increased after ATx. FLU treatment decreased by 75% 24 h after ATx.

HO-1 is an endoplasmic reticulum-localized stress-responsive enzyme, with potent antioxidant, anti-inflammatory, and anti-apoptotic properties (113). Recent studies

showed that HO-1 expression in monocytes/macrophage it beneficial in the protection against inflammation (114). Moreover, it was shown that HO-1-deficient mice are more vulnerable to IRI-induced renal damage, leading to severe early inflammation with significantly higher levels of pro-inflammatory IL-6 and low levels of the anti-inflammatory IL-10, oxidative stress, and impaired tubular regeneration with increased fibrosis within one week (115,116). In our study, we observed reduced Hmox1 mRNA expression in FLU-treated kidneys, indicating milder injury; however, HO-1 is likely not involved in S1R-mediated renoprotection.

FLU is highly lipophilic, allowing it to readily cross the BBB and quickly reach therapeutic concentrations in the brain (117). Although its CNS activity might provide added benefits during renal transplantation—particularly given the link between depression and poorer graft survival in kidney recipients—it also raises concerns about possible adverse psychoactive effects (118). Therefore, we designed a novel S1R agonist, called VCC904125 with limited BBB penetration to minimize CNS effects and we tested its renoprotective effect using *in vitro*, *in vivo*, and *ex vivo* experiments.

VCC904125 was designed as a FLU analog with increased polarity to reduce BBB permeability. The radioligand binding assay showed that VCC904125 has a similarly high affinity and slightly lower specificity for S1R than FLU (119). One of the key parts of drug development it is to identify safe and effective therapeutic candidates before they reach clinical use. Unexpected toxicities remain a leading cause of attrition during preclinical and phase I trials (120). Among these, cardiac safety is particularly critical since drug-induced cardiotoxicity is a major driver of early clinical failure. Among the first and most important evaluations is the assessment of hERG channel activity, since inhibition of this channel can prolong the QT interval and trigger dangerous arrhythmias (121). Our results revealed that VCC904125' has low hERG activity, suggesting that this original compound would offer a favorable cardiac safety profile.

In the *in vivo* experiment, a renal IRI model was used, where we showed that a single injection of the novel S1R agonist compound VCC904125 prior to the ischemic insult mitigates renal functional impairment and ameliorates structural damage 24 h after reperfusion. Both KIM-1 and NGAL levels were significantly reduced in the kidneys of VCC904125-treated animals, indicating better preserved graft organ integrity and improved tubular function. Ischemic injury in the corticomedullary region typically

manifests as ATN, histologically characterized by loss of the proximal tubular brush border, cellular swelling, and necrosis of tubular epithelial cells (122). In our experiment, S1R agonist VCC904125 treatment alleviated ATN by significantly reducing the number of tubules exhibiting irreversible damage. To demonstrate that the renoprotective effect is mediated by S1R, we performed an experiment using $S1R^{-/-}$ mice. Here, we did not observe any beneficial effects of VCC904125.

To address the growing gap between organ demand and availability, many countries have expanded their donor pools by accepting grafts from ECD and DCD (123). Unfortunately, several studies reported that this type of renal allografts carried a higher risk of DGF, primary nonfunction, and acute rejection with chronic graft failure (124). Also, it was shown that urine production and filtration capacity are often reduced in these grafts, which increases post-transplant complications and mortality (125,126).

Large cohort studies support this: Kayler et al. demonstrated in more than 18,000 transplant recipients that even a ≥1-hour increase in CI time significantly raises the risk of DGF, while Ojo et al. reported a 23% increase in DGF for every additional 6 hours of CI at 4 °C (127–129). SCS has been the traditional method and, to date, remains the gold standard for renal graft preservation, due to its availability and its superiority in lowering metabolism and preserving viability (126). For these reasons, SCS was used as the preservation technique in the present study. Conversely, hypothermia can reduce ATP production and Na+/K+-ATPase activity, leading to mitochondrial dysfunction and osmotic imbalance, which collectively promote renal cell injury and death (130). In our experiment, even 2 h of CI caused significant histological injury and apoptosis, but with the addition of S1R agonist FLU to the preservation solution, injury after 24 h of CI was similar to that after just 2 h without FLU. This renoprotective effect was not observed in $S1R^{-/-}$ mice, confirming that S1R directly mediates these mechanisms. Further, we investigated that the novel S1R agonist VCC904125 can similarly attenuate cold storage–induced renal injury. For this, we supplemented the commercially available Custodiol HTK preservation solution with VCC904125 and assessed ischemic injury after 24 h of static cold storage. The result showed no signs of severe pathological changes; however, even minor improvements during preservation may significantly enhance graft survival. Based on these results, we demonstrate that supplementing preservation solutions with

S1R agonists extends storage time without inducing additional injury, thereby improving graft preservation and optimizing organ condition prior to transplantation.

Allografts during KTx, are exposed to tubular hypoxia and ischemia arising from impaired microcirculation and increased metabolic demand, and it critically contributes to tubular injury and graft dysfunction(131,132). In the cellular hypoxic response, both hypoxia-inducible factor subunits, HIF-1α and HIF-2α, are key transcriptional regulators, with HIF-1α primarily reflecting acute hypoxic stress, whereas HIF-2α is more closely associated with sustained or chronic hypoxia and vascular adaptation (134). Our previous findings have already shown that the S1R agonist FLU modulated tubular hypoxia by decreasing HIF-1α level. To explore whether the VCC904125 provides renoprotection via modulation of tubular hypoxia, we applied *in vitro* and *in vivo* experiments. In low-grade hypoxia, VCC904125 treatment significantly reduced HIF-1α expression in the HK-2 cells, while HIF-2α remained unchanged, suggesting attenuation of acute hypoxic signaling. Similar to this, both HIF-1α and HIF-2α expression were decreased 24 h after reperfusion in animals treated with VCC904125. These findings, together with previous results, suggest that S1R activation mitigates hypoxic injury in the proximal tubules.

Inflammation early after KTx is a risk factor for both kidney allograft loss and mortality, causing significant tubular damage, microvascular dysfunction, and subsequent impairment of renal function (133) (134). Several factors may induce an inflammatory state, including proinflammatory interleukins and events with cytokine storms, such as DBD and IRI with prolonged CI (135,136). In KTx-associated IRI, damaged proximal tubular cells, as well as infiltrating leukocytes and macrophages, produce pro-inflammatory cytokines and chemokines (68). This activated inflammatory cascade not only intensifies the initial tissue injury but also contributes to poorer graft recovery and long-term dysfunction (137,138).

It has been shown that S1R activation, particularly in the CNS, has an anti-inflammatory effect by modulating microglial activation and reducing pro-inflammatory cytokine release. Ooi, K. et al. demonstrated that S1R attenuates inflammation following ischemic brain injury by limiting inflammatory cell infiltration and stabilizing endoplasmic reticulum calcium homeostasis (139). In human whole-blood cultures, Rosen et al. showed that FLU moderates inflammatory responses by reducing LPS–induced IL-6 and IL-1β production (137). Similarly, Gao et al. reported that the S1R

agonist PRE-084 significantly decreased TNF and IL1B mRNA expression in LPS-stimulated murine microglial cells (140). Moreover, it was demonstrated that CaMKII directly modulates NF-κB pathways through the S1R agonist FLU or SA4503 (141).

The NF-κB pathway represents a key molecular bridge between TLR signaling and renal inflammation. In IRI under KTx, the increased expression of TLR2 and TLR4 has been associated with impaired graft function, and in some studies, acute rejection, making their activation detrimental to long-term transplant outcomes (142–144). Once TLR2 is activated, it initiates intracellular signaling cascades that promote the release of a "rapid response" transcription factor, NF-κB, from its inhibitor IκB, allowing NF-κB to translocate to the nucleus and induce the transcription of pro-inflammatory genes (145,146). To investigate this, *in vivo* experiments were performed, and we measured the mRNA expression of inflammatory mediators.

As expected, FLU attenuated CD45+ leucocyte infiltration and reduced mRNA expression of pro-inflammatory cytokine IL-1α, IL-6, and MCP-1 following ATx. In different experiments, LPS treatment and IRI markedly increased NFKB, IL1B, IL6, and TNF levels, while VCC904125 significantly halted NF-κB downstream signaling. With these results, we demonstrated that activation of the S1R decreased LPS-induced inflammation in tubular epithelial cells and significantly reduced inflammation 24 h after IRI and ATx, highlighting the therapeutic potential of S1R-targeting drugs for modulating inflammatory pathways.

In IRI-AKI, apoptosis is a key form of cell death and is generally accepted as a major contributor to DGF after transplantation (129,147). It is characterized by different morphological changes, including cell shrinkage, membrane blebbing, chromatin condensation, and fragmentation of DNA into membrane-bound apoptotic bodies (69). These processes are tightly associated to cellular stressors such as hypoxia and oxidative injury. Key regulators of the apoptotic pathway include tumor suppressor p53, the pro-apoptotic protein BAX, and the caspase family of proteases, which coordinate the initiation and execution of apoptosis (77,148). Several studies have shown that inhibiting these pathways can confer significant renal protection against IRI. Moreover, a few studies have reported a direct modulatory role of S1R activation in suppressing apoptosis. Maurice et al. demonstrated that S1R agonist OZP002 attenuated the increment of pro-apoptotic Bax protein levels in the mouse hippocampus following amyloid Aβ25–35

peptide injection (149). Also, S1R knockdown or antagonist treatment decreases cell survival and induces p53-mediated apoptosis (150). Additionally, an in vitro study by Shen et al. demonstrated that S1R inhibition leads to upregulation of Bax, Caspase-3, and Caspase-9 in microglial cells (71). In our experiments, S1R agonist FLU reduced TUNEL and Caspase-3 positive cells after both 2 and 24 h of cold storage, while VCC904125 decreased Bax and Caspase-3 levels 24 hours after IRI. Our data and the existing literature demonstrate that S1R activation by either FLU or VCC904125 reduces apoptosis, highlighting the therapeutic potential of S1R-targeting compounds for regulating apoptotic pathways.

In conclusion, our findings demonstrate that activation of the S1R by FLU or the novel compound VCC904125 attenuates renal ischemic injury and improves post-transplant outcomes in preclinical models. By identifying key inflammatory and apoptotic pathways modulated by S1R agonism, this work provides a mechanistic insight into these protective effects. Importantly, supplementing organ preservation solutions with an S1R agonist represents a clinically relevant strategy with the potential to improve graft quality during preservation and enhance transplant outcomes. These results support further translational and clinical investigations of S1R agonists as adjuncts in renal transplantation.

6. Conclusions

- S1R agonist FLU improves transplant outcomes in a rat model of KTx by reducing functional decrement, tubular injury, renal inflammation, and apoptosis
- FLU supplementation during *ex vivo* CI improved pre-transplant graft condition, thus organ preservation time could be increased without additional injury
- Novel S1R agonist VCC904125 does not cross the BBB
- Novel S1R agonist VCC904125 attenuates renal ischemic injury by targeting the primary mechanisms of apoptosis and inflammation
- Supplementing the preservation fluid with VCC904125 is renoprotective in an *ex vivo* cold CI
- The renoprotective effects of FLU and VCC904125 were confirmed to be S1R-mediated using S1R knockout mice

7. Summary

CKD is a significant global health issue affecting over 850 million people worldwide and, in its advanced stages, is associated with progressive and ultimately complete loss of renal function. Importantly, IRI-caused AKI is increasingly recognized as a key risk factor for CKD. KTx remains the gold standard treatment for improving both survival and quality of life in patients with ESRD. Transplantation-related IRI is a complex pathophysiological process characterized by endothelial dysfunction, activation of cell death programs, and increased inflammation, which contribute to delayed graft function and adversely affect long-term transplant outcomes. Given the global shortage of donor organs, optimizing graft condition prior to transplantation is therefore of critical importance.

S1R is a multifunctional ligand-regulated chaperone protein. Previously, we described the precise localization of S1R in the kidney and demonstrated that S1R agonist fluvoxamine treatment improved postischemic survival and renal function by activating AKT–mediated NO signaling. Therefore, the main goal of our studies was to investigate whether supplementation of the preservation solution with S1R agonist FLU improves transplant outcomes. We further investigated a novel, low–BBB–penetrant S1R agonist, VCC904125, hypothesizing that it reduces apoptosis and inflammation to confer renoprotection.

In this study, we showed that pretransplant perfusion and storage of donor organs supplemented with an S1R agonist FLU significantly improves transplant outcomes through the reduction of functional impairment, tubular injury, inflammatory responses, and apoptosis. Furthermore, we developed a novel S1R agonist, VCC904125, with limited blood–brain barrier penetration and using murine models of renal ischemia–reperfusion injury and *ex vivo* CI, we demonstrated its renoprotective effects by targeting the key mechanisms underlying IRI pathology, apoptosis and inflammation.

These findings identify S1R activation as a promising strategy for improving graft preservation and potentially expanding the donor pool, although further studies are needed to confirm long-term benefits and clinical applicability.

8. References

1. Lees JS, Welsh CE, Celis-Morales CA, Mackay D, Lewsey J, Gray SR, et al. Glomerular filtration rate by differing measures, albuminuria and prediction of cardiovascular disease, mortality and end-stage kidney disease. Nat Med. 2019;25(11):1753–60. doi:10.1038/s41591-019-0627-8 PubMed PMID: 31700174.

2. Kovesdy CP. Epidemiology of chronic kidney disease: an update 2022. Kidney Int Suppl (2011). 2022;12(1):7–11. doi:10.1016/j.kisu.2021.11.003 PubMed PMID: 35529086.

3. Ricardo AC, Yang W, Sha D, Appel LJ, Chen J, Krousel-Wood M, et al. Sex-Related Disparities in CKD Progression. Journal of the American Society of Nephrology. 2019;30(1).

4. Bello AK, Levin A, Lunney M, Osman MA, Ye F, Ashuntantang GE, et al. Status of care for end stage kidney disease in countries and regions worldwide: International cross sectional survey. The BMJ. 2019;367. doi:10.1136/bmj.l5873 PubMed PMID: 31672760.

5. Webster AC, Nagler E V., Morton RL, Masson P. Chronic Kidney Disease. The Lancet. 2017;389(10075):1238–52. doi:10.1016/S0140-6736(16)32064-5 PubMed PMID: 27887750.

6. Thurlow JS, Joshi M, Yan G, Norris KC, Agodoa LY, Yuan CM, et al. Global epidemiology of end-stage kidney disease and disparities in kidney replacement therapy. Am J Nephrol. 2021;52(2):98–107. doi:10.1159/000514550 PubMed PMID: 33752206.

7. Kataria A, Trasande L, Trachtman H. The effects of environmental chemicals on renal function. Nat Rev Nephrol. 2015;11(10):610–25. doi:10.1038/nrneph.2015.94 PubMed PMID: 26100504.

8. Stanifer JW, Muiru A, Jafar TH, Patel UD. Chronic kidney disease in low- and middle-income countries. Nephrology Dialysis Transplantation. 2016;31(6):868–74. doi:10.1093/ndt/gfv466 PubMed PMID: 27217391.

9. Badalà F, Nouri-mahdavi K, Raoof DA. Chronic kidney disease after acute kidney injury: A systematic review and meta-analysis. Kidney Int. 2008;144(5):724–32. doi:10.1038/ki.2011.379.Chronic PubMed PMID: 1000000221.

10. Hsu RK, Hsu C yuan. The Role of Acute Kidney Injury in Chronic Kidney Disease. Semin Nephrol. 2016;36(4):283–92. doi:10.1016/j.semnephrol.2016.05.005 PubMed PMID: 27475659.

11. Teresa K. Chen MD, MHS DH, Knicely MD ME, Grams MD PhD. Chronic Kidney Disease Diagnosis and Management. Physiol Behav. 2017;176(10):139–48. doi:10.1001/jama.2019.14745.Chronic

12. Sabanayagam C, Banu R, Lim C, Tham YC, Cheng CY, Tan G, et al. Artificial intelligence in chronic kidney disease management: a scoping review. Theranostics . 2025;15(10):4566–78. doi:10.7150/thno.108552 PubMed PMID: 40225559.

13. Wu Q, Li J, Zhao L, Liu D, Wen J, Wang Y, et al. A noninvasive model for chronic kidney disease screening and common pathological type identification from retinal images. Nature Communications . 2025;16(1). doi:10.1038/s41467-025-62273-0 PubMed PMID: 40730556.

14. Stel VS, Boenink R, Astley ME, Boerstra BA, Radunovic D, Skrunes R, et al. A comparison of the epidemiology of kidney replacement therapy between Europe and the United States: 2021 data of the ERA Registry and the USRDS. Nephrology Dialysis Transplantation. 2024;39(10):1593–603. doi:10.1093/ndt/gfae040 PubMed PMID: 38439701.

15. Kulcsár I, Wágner L RL. A magyar vesepótló kezelések 2020. évi jelentése az ERA-EDTA Regiszternek. Hypertonia és Nephrologia. 2020;4:100–5.

16. Csaba A. Országos Kórházi Főigazgatóság Szakellátás Tervezési és Elemzési Főosztály Nemzeti Vesepótló Ellátások Regisztere Tartalomjegyzék. 2024.

17. Tonelli M, Wiebe N, Knoll G, Bello A, Browne S, Jadhav D, et al. Systematic review: Kidney transplantation compared with dialysis in clinically relevant outcomes. American Journal of Transplantation. 2011;11(10):2093–109. doi:10.1111/j.1600-6143.2011.03686.x PubMed PMID: 21883901.

18. Yang F, Liao M, Wang P, Yang Z, Liu Y. The Cost-Effectiveness of Kidney Replacement Therapy Modalities: A Systematic Review of Full Economic Evaluations. Appl Health Econ Health Policy. 2021;19(2):163–80. doi:10.1007/s40258-020-00614-4 PubMed PMID: 33047212.

19. Johansen KL, Chertow GM, Gilbertson DT, Ishani A, Israni A, Ku E, et al. US Renal Data System 2022 Annual Data Report: Epidemiology of Kidney Disease in the United States. American Journal of Kidney Diseases. W.B. Saunders; 2023. p. A8–11. doi:10.1053/j.ajkd.2022.12.001 PubMed PMID: 36822739.

20. Care SK. Recommendations for Sustainable Kidney Care - European Kidney Health Alliance (EKHA). 2015;(August).

21. Abecassis M, Bartlett ST, Collins AJ, Davis CL, Delmonico FL, Friedewald JJ, et al. Kidney Transplantation as Primary Therapy for End-Stage Renal Disease: A National Kidney Foundation/Kidney Disease Outcomes Quality Initiative (NKF/KDOQI^{TM}) Conference. Clinical Journal of the American Society of Nephrology. 2008;3(2).

22. Stel VS, Boenink R, Astley ME, Boerstra BA, Radunovic D, Skrunes R, et al. A comparison of the epidemiology of kidney replacement therapy between Europe and the United States: 2021 data of the ERA Registry and the USRDS. Nephrology Dialysis Transplantation. 2024;39(10):1593–603. doi:10.1093/ndt/gfae040 PubMed PMID: 38439701.

23. Iordanous Y, Seymour N, Young A, Johnson J, Iansavichus A V., Cuerden MS, et al. Recipient outcomes for expanded criteria living kidney donors: The disconnect between current evidence and practice. American Journal of Transplantation. 2009;9(7):1558–73. doi:10.1111/j.1600-6143.2009.02671.x PubMed PMID: 19459792.

24. Legendre C, Canaud G, Martinez F. Factors influencing long-term outcome after kidney transplantation. Transplant International. 2014;27(1):19–27. doi:10.1111/tri.12217 PubMed PMID: 24138291.

25. Loupy A, Lefaucheur C, Vernerey D, Prugger C, van Huyen JPD, Mooney N, et al. Complement-Binding Anti-HLA Antibodies and Kidney-Allograft Survival.

New England Journal of Medicine. 2013;369(13):1215–26. doi:10.1056/nejmoa1302506 PubMed PMID: 24066742.

26. Lasorsa F, Rutigliano M, Milella M, d'Amati A, Crocetto F, Pandolfo SD, et al. Ischemia–Reperfusion Injury in Kidney Transplantation: Mechanisms and Potential Therapeutic Targets. Int J Mol Sci. 2024;25(8). doi:10.3390/ijms25084332 PubMed PMID: 38673917.

27. Krishnan AR, Wong G, Chapman JR, Coates PT, Russ GR, Pleass H, et al. Prolonged Ischemic Time, Delayed Graft Function, and Graft and Patient Outcomes in Live Donor Kidney Transplant Recipients. American Journal of Transplantation. 2016;16(9):2714–23. doi:10.1111/ajt.13817 PubMed PMID: 27037866.

28. Jing L, Yao L, Zhao M, Peng LP, Liu M. Organ preservation: From the past to the future. Acta Pharmacol Sin. 2018;39(5):845–57. doi:10.1038/aps.2017.182 PubMed PMID: 29565040.

29. Catena F, Coccolini F, Montori G, Vallicelli C, Amaduzzi A, Ercolani G, et al. Kidney preservation: Review of present and future perspective. Transplant Proc. 2013;45(9):3170–7. doi:10.1016/j.transproceed.2013.02.145 PubMed PMID: 24182779.

30. O'Callaghan JM, Knight SR, Morgan RD, Morris PJ. Preservation solutions for static cold storage of kidney allografts: A systematic review and meta-analysis. American Journal of Transplantation. 2012;12(4):896–906. doi:10.1111/j.1600-6143.2011.03908.x PubMed PMID: 22221739.

31. Yuan X, Theruvath AJ, Ge X, Floerchinger B, Jurisch A, García-Cardeña G, et al. Machine perfusion or cold storage in organ transplantation: indication, mechanisms, and future perspectives. Transpl Int. 2010 Jun;23(6):561–70. doi:10.1111/j.1432-2277.2009.01047.x PubMed PMID: 20074082.

32. Wszola M, Kwiatkowski A, Domagala P, Wirkowska A, Bieniasz M, Diuwe P, et al. Preservation of kidneys by machine perfusion influences gene expression and may limit ischemia/reperfusion injury. Prog Transplant. 2014 Mar;24(1):19–26. doi:10.7182/pit2014384 PubMed PMID: 24598561.

33. van Leeuwen LL, Leuvenink HGD, Olinga P, Ruigrok MJR. Shifting Paradigms for Suppressing Fibrosis in Kidney Transplants: Supplementing Perfusion Solutions With Anti-fibrotic Drugs. Front Med (Lausanne). 2022;8(January):1–12. doi:10.3389/fmed.2021.806774

34. Hoste EAJ, Kellum JA, Selby NM, Zarbock A, Palevsky PM, Bagshaw SM, et al. Global epidemiology and outcomes of acute kidney injury. Nat Rev Nephrol. 2018;14(10):607–25. doi:10.1038/s41581-018-0052-0 PubMed PMID: 30135570.

35. Lewington AJP, Cerdá J, Mehta RL. Raising awareness of acute kidney injury: A global perspective of a silent killer. Kidney Int. 2013;84(3):457–67. doi:10.1038/ki.2013.153 PubMed PMID: 23636171.

36. Radzig MA, Nadtochenko VA, Koksharova OA, Kiwi J, Lipasova VA, Khmel IA. Antibacterial effects of silver nanoparticles on gram-negative bacteria: Influence on the growth and biofilms formation, mechanisms of action. Colloids Surf B Biointerfaces. 2013;102:300–6. doi:10.1016/j.colsurfb.2012.07.039

37. Olowu WA, Niang A, Osafo C, Ashuntantang G, Arogundade FA, Porter J, et al. Outcomes of acute kidney injury in children and adults in sub-Saharan Africa: A systematic review. Lancet Glob Health. 2016;4(4):e242–50. doi:10.1016/S2214-109X(15)00322-8 PubMed PMID: 27013312.

38. Susantitaphong P, Cruz DN, Cerda J, Abulfaraj M, Alqahtani F, Koulouridis I, et al. World incidence of AKI: a meta-analysis. Clin J Am Soc Nephrol. 2013 Sep;8(9):1482–93. doi:10.2215/CJN.00710113 PubMed PMID: 23744003.

39. Kellum JA, Sileanu FE, Murugan R, Lucko N, Shaw AD, Clermont G. Classifying AKI by Urine Output versus Serum Creatinine Level. J Am Soc Nephrol. 2015 Sep;26(9):2231–8. doi:10.1681/ASN.2014070724 PubMed PMID: 25568178.

40. Gameiro J, Fonseca JA, Jorge S, Lopes JA. Acute kidney injury definition and diagnosis: A narrative review. J Clin Med. 2018;7(10):1–13. doi:10.3390/jcm7100307

41. Bellomo R, Ronco C, Kellum JA, Mehta RL, Palevsky P. Acute renal failure - definition, outcome measures, animal models, fluid therapy and information

technology needs: the Second International Consensus Conference of the Acute Dialysis Quality Initiative (ADQI) Group. Crit Care. 2004;8(4). doi:10.1186/cc2872 PubMed PMID: 15312219.

42. Mehta RL, Kellum JA, Shah S V., Molitoris BA, Ronco C, Warnock DG, et al. Acute Kidney Injury Network: Report of an initiative to improve outcomes in acute kidney injury. Crit Care. 2007;11(2):1–8. doi:10.1186/cc5713 PubMed PMID: 17331245.

43. Khwaja A. KDIGO clinical practice guidelines for acute kidney injury. Nephron Clin Pract. 2012;120(4):c179-84. doi:10.1159/000339789 PubMed PMID: 22890468.

44. Husain-Syed F, Ronco C. The odyssey of risk stratification in acute kidney injury. Nat Rev Nephrol. 2018 Nov;14(11):660–2. doi:10.1038/s41581-018-0053-z PubMed PMID: 30143788.

45. Kashani K, Kellum JA. Novel biomarkers indicating repair or progression after acute kidney injury. Curr Opin Nephrol Hypertens. 2015 Jan;24(1):21–7. doi:10.1097/MNH.0000000000000090 PubMed PMID: 25415614.

46. Ichimura T, Hung CC, Yang SA, Stevens JL, Bonventre J V. Kidney injury molecule-1: a tissue and urinary biomarker for nephrotoxicant-induced renal injury. Am J Physiol Renal Physiol. 2004 Mar;286(3):F552-63. doi:10.1152/ajprenal.00285.2002 PubMed PMID: 14600030.

47. Zou C, Wang C, Lu L. Advances in the study of subclinical AKI biomarkers. Front Physiol. 2022;13(August):1–15. doi:10.3389/fphys.2022.960059

48. Sabbisetti VS, Waikar SS, Antoine DJ, Smiles A, Wang C, Ravisankar A, et al. Blood kidney injury molecule-1 is a biomarker of acute and chronic kidney injury and predicts progression to ESRD in type I diabetes. J Am Soc Nephrol. 2014 Oct;25(10):2177–86. doi:10.1681/ASN.2013070758 PubMed PMID: 24904085.

49. Jäntti T, Tarvasmäki T, Harjola VP, Pulkki K, Turkia H, Sabell T, et al. Predictive value of plasma proenkephalin and neutrophil gelatinase-associated lipocalin in

acute kidney injury and mortality in cardiogenic shock. Ann Intensive Care. 2021;11(1). doi:10.1186/s13613-021-00814-8

50. Schinstock CA, Semret MH, Wagner SJ, Borland TM, Bryant SC, Kashani KB, et al. Urinalysis is more specific and urinary neutrophil gelatinase-associated lipocalin is more sensitive for early detection of acute kidney injury. Nephrol Dial Transplant. 2013 May;28(5):1175–85. doi:10.1093/ndt/gfs127 PubMed PMID: 22529161.

51. Su Y, Gong Z, Wu Y, Tian Y, Liao X. Diagnostic value of urine tissue inhibitor of metalloproteinase-2 and insulin-like growth factor-binding protein 7 for acute kidney injury: A meta-analysis. PLoS One. 2017;12(1):1–14. doi:10.1371/journal.pone.0170214 PubMed PMID: 28107490.

52. Ko GJ, Grigoryev DN, Linfert D, Jang HR, Watkins T, Cheadle C, et al. Transcriptional analysis of kidneys during repair from AKI reveals possible roles for NGAL and KIM-1 as biomarkers of AKI-to-CKD transition. Am J Physiol Renal Physiol. 2010 Jun;298(6):F1472-83. doi:10.1152/ajprenal.00619.2009 PubMed PMID: 20181666.

53. Devarajan P. Biomarkers for the early detection of acute kidney injury. Curr Opin Pediatr. 2011 Apr;23(2):194–200. doi:10.1097/MOP.0b013e328343f4dd PubMed PMID: 21252674.

54. Bihorac A, Kellum JA. Acute kidney injury in 2014: A step towards understanding mechanisms of renal repair. Nat Rev Nephrol. 2015;11(2):74–5. doi:10.1038/nrneph.2014.245 PubMed PMID: 25561080.

55. Kashani K, Al-Khafaji A, Ardiles T, Artigas A, Bagshaw SM, Bell M, et al. Discovery and validation of cell cycle arrest biomarkers in human acute kidney injury. Crit Care. 2013;17(1):1–12. doi:10.1186/cc12503 PubMed PMID: 23388612.

56. Bhosale SJ, Kulkarni AP. Biomarkers in acute kidney injury. Indian Journal of Critical Care Medicine. 2020;24:S90–3. doi:10.5005/jp-journals-10071-23398

57. Zuk A, Bonventre J V. Acute Kidney Injury. Annu Rev Med. 2016 Jan 14;67(1):293–307. doi:10.1146/annurev-med-050214-013407

58. Gaut JP, Liapis H. Acute kidney injury pathology and pathophysiology: A retrospective review. Clin Kidney J. 2021;14(2):526–36. doi:10.1093/ckj/sfaa142

59. Shiva N, Sharma N, Kulkarni YA, Mulay SR, Gaikwad AB. Renal ischemia/reperfusion injury: An insight on in vitro and in vivo models. Life Sci. 2020;256(April):117860. doi:10.1016/j.lfs.2020.117860 PubMed PMID: 32534037.

60. Nieuwenhuijs-Moeke GJ, Pischke SE, Berger SP, Sanders JSF, Pol RA, Struys MMRF, et al. Ischemia and reperfusion injury in kidney transplantation: Relevant mechanisms in injury and repair. J Clin Med. 2020;9(1). doi:10.3390/jcm9010253

61. Kako K, Kato M, Matsuoka T, Mustapha A. Depression of membrane-bound Na+-K+-ATPase activity induced by free radicals and by ischemia of kidney. Am J Physiol. 1988 Feb;254(2 Pt 1):C330-7. doi:10.1152/ajpcell.1988.254.2.C330 PubMed PMID: 2831728.

62. Sugiyama S, Hanaki Y, Ogawa T, Hieda N, Taki K, Ozawa T. The effects of SUN 1165, a novel sodium channel blocker, on ischemia-induced mitochondrial dysfunction and leakage of lysosomal enzymes in canine hearts. Biochem Biophys Res Commun. 1988 Dec;157(2):433–9. doi:10.1016/s0006-291x(88)80267-5 PubMed PMID: 2849430.

63. Edelstein CL, Ling H, Schrier RW. The nature of renal cell injury. Kidney Int. 1997 May;51(5):1341–51. doi:10.1038/ki.1997.183 PubMed PMID: 9150442.

64. Park M, Kwon CH, Ha HK, Han M, Song SH. RNA-Seq identifies condition-specific biological signatures of ischemia-reperfusion injury in the human kidney. BMC Nephrol. 2020;21(Suppl 1):1–12. doi:10.1186/s12882-020-02025-y PubMed PMID: 32977749.

65. Ponticelli C. Ischaemia-reperfusion injury: a major protagonist in kidney transplantation. Nephrol Dial Transplant. 2014;29:1134–40. doi:10.1093/ndt/gft488

66. Layton AT, Vallon V, Edwards A. Modeling oxygen consumption in the proximal tubule: effects of NHE and SGLT2 inhibition. Am J Physiol Renal Physiol. 2015 Jun;308(12):F1343-57. doi:10.1152/ajprenal.00007.2015 PubMed PMID: 25855513.

67. Bonventre J V, Yang L. Cellular pathophysiology of ischemic acute kidney injury Find the latest version : Science in medicine Cellular pathophysiology of ischemic acute kidney injury. J Clin Invest. 2011;121(11):4210–21. doi:10.1172/JCI45161.4210 PubMed PMID: 22045571.

68. Sharfuddin AA, Molitoris BA. Pathophysiology of ischemic acute kidney injury. Nat Rev Nephrol. 2011 Apr;7(4):189–200. doi:10.1038/nrneph.2011.16 PubMed PMID: 21364518.

69. Li C, Yu Y, Zhu S, Hu Y, Ling X, Xu L, et al. The emerging role of regulated cell death in ischemia and reperfusion-induced acute kidney injury: current evidence and future perspectives. Cell Death Discov. 2024;10(1):1–10. doi:10.1038/s41420-024-01979-4

70. Eibel H, Kraus H, Sic H, Kienzler AK, Rizzi M. B cell biology: an overview. Curr Allergy Asthma Rep. 2014 May;14(5):434. doi:10.1007/s11882-014-0434-8 PubMed PMID: 24633618.

71. Park JS, Svetkauskaite D, He Q, Kim JY, Strassheim D, Ishizaka A, et al. Involvement of Toll-like Receptors 2 and 4 in Cellular Activation by High Mobility Group Box 1 Protein. Journal of Biological Chemistry. 2004;279(9):7370–7. doi:10.1074/jbc.M306793200 PubMed PMID: 14660645.

72. Singbartl K, Green SA, Ley K. Blocking P-selectin protects from ischemia/reperfusion-induced acute renal failure. FASEB J. 2000 Jan;14(1):48–54. doi:10.1096/fasebj.14.1.48 PubMed PMID: 10627279.

73. Kelly KJ, Williams WWJ, Colvin RB, Meehan SM, Springer TA, Gutierrez-Ramos JC, et al. Intercellular adhesion molecule-1-deficient mice are protected against ischemic renal injury. J Clin Invest. 1996 Feb;97(4):1056–63. doi:10.1172/JCI118498 PubMed PMID: 8613529.

74. Schofield ZV, Woodruff TM, Halai R, Wu MCL, Cooper MA. Neutrophils--a key component of ischemia-reperfusion injury. Shock. 2013 Dec;40(6):463–70. doi:10.1097/SHK.0000000000000044 PubMed PMID: 24088997.

75. Ma S, Wang DH. Knockout of Trpa1 Exacerbates Renal Ischemia-Reperfusion Injury With Classical Activation of Macrophages. Am J Hypertens. 2021 Feb;34(1):110–6. doi:10.1093/ajh/hpaa162 PubMed PMID: 33005917.

76. Hasegawa S, Inoue T, Nakamura Y, Fukaya D, Uni R, Wu CH, et al. Activation of sympathetic signaling in macrophages blocks systemic inflammation and protects against renal ischemia-reperfusion injury. Journal of the American Society of Nephrology. 2021;32(7):1599–615. doi:10.1681/ASN.2020121723 PubMed PMID: 33875568.

77. Galluzzi L, Vitale I, Aaronson SA, Abrams JM, Adam D, Agostinis P, et al. Molecular mechanisms of cell death: recommendations of the Nomenclature Committee on Cell Death 2018. Cell Death Differ. 2018 Mar;25(3):486–541. doi:10.1038/s41418-017-0012-4 PubMed PMID: 29362479.

78. Hanner M, Moebius FF, Flandorfer A, Knaus HG, Striessnig J, Kempner E, et al. Purification, molecular cloning, and expression of the mammalian sigma1-binding site. Proc Natl Acad Sci U S A. 1996 Jul;93(15):8072–7. doi:10.1073/pnas.93.15.8072 PubMed PMID: 8755605.

79. Rousseaux CG, Greene SF. Sigma receptors [σRs]: biology in normal and diseased states. J Recept Signal Transduct Res. 2016 Aug;36(4):327–88. doi:10.3109/10799893.2015.1015737 PubMed PMID: 26056947.

80. Chu UB, Ruoho AE. Biochemical Pharmacology of the Sigma-1 Receptor. Mol Pharmacol. 2016 Jan 1;89(1):142–53. doi:10.1124/MOL.115.101170 PubMed PMID: 26560551.

81. Kekuda R, Prasad PD, Fei YJ, Leibach FH, Ganapathy V. Cloning and functional expression of the human type 1 sigma receptor (hSigmaR1). Biochem Biophys Res Commun. 1996 Dec;229(2):553–8. doi:10.1006/bbrc.1996.1842 PubMed PMID: 8954936.

82. Mei J, Pasternak GW. Molecular cloning and pharmacological characterization of the rat sigma1 receptor. Biochem Pharmacol. 2001 Aug;62(3):349–55. doi:10.1016/s0006-2952(01)00666-9 PubMed PMID: 11434908.

83. Hayashi T, Su TP. Sigma-1 receptor chaperones at the ER-mitochondrion interface regulate Ca(2+) signaling and cell survival. Cell. 2007 Nov;131(3):596–610. doi:10.1016/j.cell.2007.08.036 PubMed PMID: 17981125.

84. Ortega-Roldan JL, Ossa F, Schnell JR. Characterization of the human sigma-1 receptor chaperone domain structure and binding immunoglobulin protein (BiP) interactions. J Biol Chem. 2013 Jul;288(29):21448–57. doi:10.1074/jbc.M113.450379 PubMed PMID: 23760505.

85. Hayashi T. The sigma-1 receptor in cellular stress signaling. Frontiers in Neuroscience. Frontiers Media S.A.; 2019. doi:10.3389/fnins.2019.00733

86. Ryskamp DA, Korban S, Zhemkov V, Kraskovskaya N, Bezprozvanny I. Neuronal sigma-1 receptors: Signaling functions and protective roles in neurodegenerative diseases. Front Neurosci. 2019;13(AUG):1–20. doi:10.3389/fnins.2019.00862

87. Aishwarya R, Abdullah CS, Morshed M, Remex NS, Bhuiyan MS. Sigmar1's Molecular, Cellular, and Biological Functions in Regulating Cellular Pathophysiology. Frontiers in Physiology. Frontiers Media S.A.; 2021. doi:10.3389/fphys.2021.705575

88. Nguyen L, Lucke-Wold BP, Mookerjee SA, Cavendish JZ, Robson MJ, Scandinaro AL, et al. Role of sigma-1 receptors in neurodegenerative diseases. J Pharmacol Sci. 2015;127(1):17–29. doi:10.1016/j.jphs.2014.12.005 PubMed PMID: 25704014.

89. Francardo V, Bez F, Wieloch T, Nissbrandt H, Ruscher K, Cenci MA. Pharmacological stimulation of sigma-1 receptors has neurorestorative effects in experimental parkinsonism. Brain. 2014 Jul;137(Pt 7):1998–2014. doi:10.1093/brain/awu107 PubMed PMID: 24755275.

90. Francardo V, Geva M, Bez F, Denis Q, Steiner L, Hayden MR, et al. Pridopidine Induces Functional Neurorestoration Via the Sigma-1 Receptor in a Mouse Model

of Parkinson's Disease. Neurotherapeutics. 2019 Apr;16(2):465–79. doi:10.1007/s13311-018-00699-9 PubMed PMID: 30756361.

91. Gao QJ, Yang B, Chen J, Shi SB, Yang HJ, Liu X. Sigma-1 Receptor Stimulation with PRE-084 Ameliorates Myocardial Ischemia-Reperfusion Injury in Rats. Chin Med J (Engl). 2018 Mar;131(5):539–43. doi:10.4103/0366-6999.226076 PubMed PMID: 29483387.

92. Fo Y, Zhang C, Chen X, Liu X, Ye T, Guo Y, et al. Chronic sigma-1 receptor activation ameliorates ventricular remodeling and decreases susceptibility to ventricular arrhythmias after myocardial infarction in rats. Eur J Pharmacol. 2020 Dec;889:173614. doi:10.1016/j.ejphar.2020.173614 PubMed PMID: 33010304.

93. Kryzhanovskii SA, Tsorin IB, Stolyaruk VN, Vititnova MB, Ionova EO, Barchukov V V, et al. Examination of Cardioprotective Effects of Fabomotizole Hydrochloride in Translational Rat Model of Chronic Heart Failure. Bull Exp Biol Med. 2019 Nov;168(1):33–7. doi:10.1007/s10517-019-04639-1 PubMed PMID: 31741244.

94. Hosszu A, Antal Z, Lenart L, Hodrea J, Koszegi S, Balogh DB, et al. s1-Receptor Agonism Protects against Renal Ischemia-Reperfusion Injury. J Am Soc Nephrol. 2017;28:152–65. doi:10.1681/ASN.2015070772

95. Milardović I, Vitlov Uljević M, Vukojević K, Kostić S, Filipović N. Renal expression of sigma 1 receptors in diabetic rats. Acta Histochem. 2020 Sep;122(6):151580. doi:10.1016/j.acthis.2020.151580 PubMed PMID: 32778242.

96. Hosszu A, Antal Z, Veres-Szekely A, Lenart L, Balogh DB, Szkibinszkij E, et al. The role of Sigma-1 receptor in sex-specific heat shock response in an experimental rat model of renal ischaemia/reperfusion injury. Transplant International. 2018;31(11):1268–78. doi:10.1111/tri.13293 PubMed PMID: 29908082.

97. Hashimoto K. Activation of sigma-1 receptor chaperone in the treatment of neuropsychiatric diseases and its clinical implication. J Pharmacol Sci. 2015 Jan;127(1):6–9. doi:10.1016/j.jphs.2014.11.010 PubMed PMID: 25704012.

98. Cobos EJ, Entrena JM, Nieto FR, Cendán CM, Del Pozo E. Pharmacology and therapeutic potential of sigma(1) receptor ligands. Curr Neuropharmacol. 2008 Dec;6(4):344–66. doi:10.2174/157015908787386113 PubMed PMID: 19587856.

99. Balogh DB, Hodrea J, Saeed A, Cserhalmi M, Rozsahegyi A, Lakat T, et al. Sigma-1 Receptor as a Novel Therapeutic Target in Diabetic Kidney Disease. Int J Mol Sci. 2024;25(24):1–15. doi:10.3390/ijms252413327 PubMed PMID: 39769092.

100. Lazarou C, Moysidou E, Christodoulou M, Stai S, Lioulios G, Kasimatis E, et al. Protocol Biopsies in Kidney Transplant Recipients: Current Practice After Much Discussion. Biomedicines. 2025 Jul;13(7). doi:10.3390/biomedicines13071660 PubMed PMID: 40722731.

101. Mohan S, Campenot E, Chiles MC, Santoriello D, Bland E, Crew RJ, et al. Association between Reperfusion Renal Allograft Biopsy Findings and Transplant Outcomes. J Am Soc Nephrol. 2017 Oct;28(10):3109–17. doi:10.1681/ASN.2016121330 PubMed PMID: 28684646.

102. Wang M, Lv J, Zhao J, Wang H, Chen J, Wu J. Postreperfusion Renal Allograft Biopsy Predicts Outcome of Single-Kidney Transplantation: A 10-Year Observational Study in China. Kidney Int Rep. 2024 Jan;9(1):96–107. doi:10.1016/j.ekir.2023.10.021 PubMed PMID: 38312778.

103. Naesens M. Zero-Time Renal Transplant Biopsies: A Comprehensive Review. Transplantation. 2016 Jul;100(7):1425–39. doi:10.1097/TP.0000000000001018 PubMed PMID: 26599490.

104. Schumann-Bischoff A, Schmitz J, Scheffner I, Schmitt R, Broecker V, Haller H, et al. Distinct morphological features of acute tubular injury in renal allografts correlate with clinical outcome. Am J Physiol Renal Physiol. 2018 Sep;315(3):F701–10. doi:10.1152/ajprenal.00189.2017 PubMed PMID: 29638160.

105. Duffield JS, Park KM, Hsiao LL, Kelley VR, Scadden DT, Ichimura T, et al. Restoration of tubular epithelial cells during repair of the postischemic kidney occurs independently of bone marrow-derived stem cells. J Clin Invest. 2005 Jul;115(7):1743–55. doi:10.1172/JCI22593 PubMed PMID: 16007251.

106. Venkatachalam MA, Weinberg JM, Kriz W, Bidani AK. Failed Tubule Recovery, AKI-CKD Transition, and Kidney Disease Progression. J Am Soc Nephrol. 2015 Aug;26(8):1765–76. doi:10.1681/ASN.2015010006 PubMed PMID: 25810494.

107. Dixon Thomas1, Seeba Zachariah1, Abdelgadir Elamin Eltom Elamin2 ALOH. Limitations of serum creatinine as a marker of renal function. Scholars Academic Journal of Pharmacy (SAJP). 2017;6(7):320–9. doi:10.21276/sajp

108. Tholén M, Lannemyr L, Møller-Sørensen H, Ricksten SE. Serum creatinine is an unreliable marker of renal function in patients undergoing heart transplantation. Acta Anaesthesiol Scand. 2024 May;68(5):619–25. doi:10.1111/aas.14397 PubMed PMID: 38411237.

109. Quang TH, Nguyet MP, Thao DP, Thi MH, Phuong Thi Dam L, Thi HH, et al. Evaluation of Urinary Neutrophil Gelatinase Associated Lipocalin and Kidney Injury Molecule-1 as Diagnostic Markers for Early Nephropathy in Patients with Type 2 Diabetes Mellitus. Diabetes Metab Syndr Obes. 2020;13:2199–207. doi:10.2147/DMSO.S258678 PubMed PMID: 32612375.

110. Vaidya VS, Ozer JS, Dieterle F, Collings FB, Ramirez V, Troth S, et al. Kidney injury molecule-1 outperforms traditional biomarkers of kidney injury in preclinical biomarker qualification studies. Nat Biotechnol. 2010 May;28(5):478–85. doi:10.1038/nbt.1623 PubMed PMID: 20458318.

111. Liu J, Krautzberger AM, Sui SH, Hofmann OM, Chen Y, Baetscher M, et al. Cell-specific translational profiling in acute kidney injury. J Clin Invest. 2014 Mar;124(3):1242–54. doi:10.1172/JCI72126 PubMed PMID: 24569379.

112. Maier HT, Ashraf MI, Denecke C, Weiss S, Augustin F, Messner F, et al. Prediction of delayed graft function and long-term graft survival by serum and urinary neutrophil gelatinase-associated lipocalin during the early postoperative phase after kidney transplantation. PLoS One. 2018;13(1):e0189932. doi:10.1371/journal.pone.0189932 PubMed PMID: 29304176.

113. Bolisetty S, Zarjou A, Agarwal A. Heme Oxygenase 1 as a Therapeutic Target in Acute Kidney Injury. Am J Kidney Dis. 2017 Apr;69(4):531–45. doi:10.1053/j.ajkd.2016.10.037 PubMed PMID: 28139396.

114. Li Y, Ma K, Han Z, Chi M, Sai X, Zhu P, et al. Immunomodulatory Effects of Heme Oxygenase-1 in Kidney Disease. Front Med (Lausanne). 2021;8:708453. doi:10.3389/fmed.2021.708453 PubMed PMID: 34504854.

115. Tracz MJ, Juncos JP, Croatt AJ, Ackerman AW, Grande JP, Knutson KL, et al. Deficiency of heme oxygenase-1 impairs renal hemodynamics and exaggerates systemic inflammatory responses to renal ischemia. Kidney Int. 2007 Nov;72(9):1073–80. doi:10.1038/sj.ki.5002471 PubMed PMID: 17728706.

116. Rossi M, Thierry A, Delbauve S, Preyat N, Soares MP, Roumeguère T, et al. Specific expression of heme oxygenase-1 by myeloid cells modulates renal ischemiareperfusion injury. Sci Rep. 2017;7(1):1–14. doi:10.1038/s41598-017-00220-w PubMed PMID: 28298633.

117. Hallifax D, Houston JB. Saturable uptake of lipophilic amine drugs into isolated hepatocytes: mechanisms and consequences for quantitative clearance prediction. Drug Metab Dispos. 2007 Aug;35(8):1325–32. doi:10.1124/dmd.107.015131 PubMed PMID: 17470525.

118. Ebert D, Albert R, May A, Merz A, Murata H, Stosiek I, et al. The serotonin syndrome and psychosis-like side-effects of fluvoxamine clinical use--an estimation of incidence. Eur Neuropsychopharmacol. 1997 Feb;7(1):71–4. doi:10.1016/s0924-977x(96)00043-0 PubMed PMID: 9088888.

119. Tagashira H, Bhuiyan S, Shioda N, Hasegawa H, Kanai H, Fukunaga K. Sigma1-receptor stimulation with fluvoxamine ameliorates transverse aortic constriction-induced myocardial hypertrophy and dysfunction in mice. Am J Physiol Heart Circ Physiol. 2010 Nov;299(5):H1535-45. doi:10.1152/ajpheart.00198.2010 PubMed PMID: 20802134.

120. Singh N, Vayer P, Tanwar S, Poyet JL, Tsaioun K, Villoutreix BO. Drug discovery and development: introduction to the general public and patient groups. Frontiers in Drug Discovery. 2023;3(May):1–11. doi:10.3389/fddsv.2023.1201419

121. Stergiopoulos C, Tsopelas F, Valko K. Prediction of hERG inhibition of drug discovery compounds using biomimetic HPLC measurements. ADMET DMPK. 2021;9(3):191–207. doi:10.5599/admet.995 PubMed PMID: 35300361.

122. Bugno G. Nephrology Acute Tubular Necrosis : A Comprehensive Exploration of Causes , Symptoms , Diagnosis , and Treatment Options for Impaired Renal Function. Vol. 6. 2023;6:6–8. doi:10.47532/oain.2023.6(3).76-78

123. Boenink R, Kramer A, Tuinhout RE, Savoye E, Åsberg A, Idrizi A, et al. Trends in kidney transplantation rate across Europe: study from the ERA Registry. Nephrol Dial Transplant. 2023 May;38(6):1528–39. doi:10.1093/ndt/gfac333 PubMed PMID: 36610723.

124. Lucarelli G, Bettocchi C, Battaglia M, Impedovo S V, Vavallo A, Grandaliano G, et al. Extended criteria donor kidney transplantation: comparative outcome analysis between single versus double kidney transplantation at 5 years. Transplant Proc. 2010 May;42(4):1104–7. doi:10.1016/j.transproceed.2010.03.059 PubMed PMID: 20534234.

125. de Vries EE, Snoeijs MG, van Heurn E. Kidney donation from children after cardiac death. Crit Care Med. 2010 Jan;38(1):249–53. doi:10.1097/CCM.0b013e3181c025fd PubMed PMID: 19851095.

126. Abou Taka M, Dugbartey GJ, Sener A. The Optimization of Renal Graft Preservation Temperature to Mitigate Cold Ischemia-Reperfusion Injury in Kidney Transplantation. Int J Mol Sci. 2022 Dec;24(1). doi:10.3390/ijms24010567 PubMed PMID: 36614006.

127. Barba J, Zudaire JJ, Robles JE, Tienza A, Rosell D, Berián JM, et al. [Is there a safe cold ischemia time interval for the renal graft?]. Actas Urol Esp. 2011 Sep;35(8):475–80. doi:10.1016/j.acuro.2011.03.005 PubMed PMID: 21550140.

128. Kayler LK, Srinivas TR, Schold JD. Influence of CIT-induced DGF on kidney transplant outcomes. Am J Transplant. 2011 Dec;11(12):2657–64. doi:10.1111/j.1600-6143.2011.03817.x PubMed PMID: 22051325.

129. Ojo AO, Wolfe RA, Held PJ, Port FK, Schmouder RL. DELAYED GRAFT FUNCTION: RISK FACTORS AND IMPLICATIONS FOR RENAL ALLOGRAFT SURVIVAL1. Transplantation. 1997;63(7).

130. Dragun D, Hoff U, Park JK, Qun Y, Schneider W, Luft FC, et al. Prolonged cold preservation augments vascular injury independent of renal transplant immunogenicity and function. Kidney Int. 2001 Sep;60(3):1173–81. doi:10.1046/j.1523-1755.2001.0600031173.x PubMed PMID: 11532114.

131. Conde E, Alegre L, Blanco-Sánchez I, Sáenz-Morales D, Aguado-Fraile E, Ponte B, et al. Hypoxia inducible factor 1-alpha (hif-1 alpha) is induced during reperfusion after renal ischemia and is critical for proximal tubule cell survival. PLoS One. 2012;7(3). doi:10.1371/journal.pone.0033258 PubMed PMID: 22432008.

132. Akhtar MZ, Sutherland AI, Huang H, Ploeg RJ, Pugh CW. The role of hypoxia-inducible factors in organ donation and transplantation: The current perspective and future opportunities. American Journal of Transplantation. 2014;14(7):1481–7. doi:10.1111/ajt.12737 PubMed PMID: 24909061.

133. Kinsey GR, Li L, Okusa MD. Inflammation in acute kidney injury. Nephron Exp Nephrol. 2008;109(4):e102-7. doi:10.1159/000142934 PubMed PMID: 18802372.

134. Abedini S, Holme I, März W, Weihrauch G, Fellström B, Jardine A, et al. Inflammation in renal transplantation. Clin J Am Soc Nephrol. 2009 Jul;4(7):1246–54. doi:10.2215/CJN.00930209 PubMed PMID: 19541816.

135. Tonelli M, Sacks F, Pfeffer M, Jhangri GS, Curhan G. Biomarkers of inflammation and progression of chronic kidney disease. Kidney Int. 2005 Jul;68(1):237–45. doi:10.1111/j.1523-1755.2005.00398.x PubMed PMID: 15954913.

136. Debout A, Foucher Y, Trébern-Launay K, Legendre C, Kreis H, Mourad G, et al. Each additional hour of cold ischemia time significantly increases the risk of graft failure and mortality following renal transplantation. Kidney Int. 2015 Feb;87(2):343–9. doi:10.1038/ki.2014.304 PubMed PMID: 25229341.

137. Rosen DA, Seki SM, Fernández-Castañeda A, Beiter RM, Eccles JD, Woodfolk JA, et al. Modulation of the sigma-1 receptor-IRE1 pathway is beneficial in preclinical models of inflammation and sepsis. Sci Transl Med. 2019 Feb;11(478). doi:10.1126/scitranslmed.aau5266 PubMed PMID: 30728287.

138. Rafiee L, Hajhashemi V, Javanmard SH. Fluvoxamine inhibits some inflammatory genes expression in LPS/stimulated human endothelial cells, U937 macrophages, and carrageenan-induced paw edema in rat. Iran J Basic Med Sci. 2016 Sep;19(9):977–84. PubMed PMID: 27803785.

139. Ooi K, Hu L, Feng Y, Han C, Ren X, Qian X, et al. Sigma-1 Receptor Activation Suppresses Microglia M1 Polarization via Regulating Endoplasmic Reticulum-Mitochondria Contact and Mitochondrial Functions in Stress-Induced Hypertension Rats. Mol Neurobiol. 2021 Dec;58(12):6625–46. doi:10.1007/s12035-021-02488-6 PubMed PMID: 34601668.

140. Gao T, Gao C, Liu Z, Wang Y, Jia X, Tian H, et al. Inhibition of Noncanonical Ca(2+) Oscillation/Calcineurin/GSK-3β Pathway Contributes to Anti-Inflammatory Effect of Sigma-1 Receptor Activation. Neurochem Res. 2022 Feb;47(2):264–78. doi:10.1007/s11064-021-03439-2 PubMed PMID: 34468932.

141. Moriguchi S, Sakagami H, Yabuki Y, Sasaki Y, Izumi H, Zhang C, et al. Stimulation of Sigma-1 Receptor Ameliorates Depressive-like Behaviors in CaMKIV Null Mice. Mol Neurobiol. 2015 Dec;52(3):1210–22. doi:10.1007/s12035-014-8923-2 PubMed PMID: 25316382.

142. Wu H, Chen G, Wyburn KR, Yin J, Bertolino P, Eris JM, et al. TLR4 activation mediates kidney ischemia/reperfusion injury. J Clin Invest. 2007 Oct;117(10):2847–59. doi:10.1172/JCI31008 PubMed PMID: 17853945.

143. Tsuboi N, Yoshikai Y, Matsuo S, Kikuchi T, Iwami KI, Nagai Y, et al. Roles of toll-like receptors in C-C chemokine production by renal tubular epithelial cells. J Immunol. 2002 Aug;169(4):2026–33. doi:10.4049/jimmunol.169.4.2026 PubMed PMID: 12165529.

144. Leemans JC, Butter LM, Pulskens WPC, Teske GJD, Claessen N, van der Poll T, et al. The role of Toll-like receptor 2 in inflammation and fibrosis during

progressive renal injury. PLoS One. 2009 May;4(5):e5704. doi:10.1371/journal.pone.0005704 PubMed PMID: 19479087.

145. O'Neill LAJ. How Toll-like receptors signal: what we know and what we don't know. Curr Opin Immunol. 2006 Feb;18(1):3–9. doi:10.1016/j.coi.2005.11.012 PubMed PMID: 16343886.

146. Liew FY, Xu D, Brint EK, O'Neill LAJ. Negative regulation of Toll-like receptor-mediated immune responses. Nat Rev Immunol. 2005;5(6):446–58. doi:10.1038/nri1630

147. Havasi A, Borkan SC. Apoptosis and acute kidney injury. Kidney Int. 2011 Jul;80(1):29–40. doi:10.1038/ki.2011.120 PubMed PMID: 21562469.

148. Kruiswijk F, Labuschagne CF, Vousden KH. p53 in survival, death and metabolic health: a lifeguard with a licence to kill. Nat Rev Mol Cell Biol. 2015 Jul;16(7):393–405. doi:10.1038/nrm4007 PubMed PMID: 26122615.

149. Maurice T, Volle JN, Strehaiano M, Crouzier L, Pereira C, Kaloyanov N, et al. Neuroprotection in non-transgenic and transgenic mouse models of Alzheimer's disease by positive modulation of σ1 receptors. Pharmacol Res. 2019 Jun 1;144:315–30. doi:10.1016/J.PHRS.2019.04.026 PubMed PMID: 31048034.

150. Happy M, Dejoie J, Zajac CK, Cortez B, Chakraborty K, Aderemi J, et al. Sigma 1 Receptor antagonist potentiates the anti-cancer effect of p53 by regulating ER stress, ROS production, Bax levels, and caspase-3 activation. Biochem Biophys Res Commun. 2015 Jan;456(2):683–8. doi:10.1016/j.bbrc.2014.12.029 PubMed PMID: 25511708.

9. Bibliography of the candidate's publications

Publications related to the theme of the PhD thesis

Akos R. Toth, Tamas Lakat, Andras Budai, Hanga Kallay, Balint Szokol, Laszlo J. Wagner, Laszlo Orfi, Marcell Kreko, Attila J. Szabo, Andrea Fekete & Adam Hosszu; Novel Sigma-1 receptor agonist alleviates renal ischemic injury by targeting apoptotic and inflammatory pathways, Scientific Reports 2025, **IF= 3.9**

Adam Hosszu, **Akos R Toth**, Tamas Lakat, Ganna Stepanova, Zsuzsanna Antal, Laszlo J Wagner, Attila J Szabo, Andrea Fekete; The Sigma-1 Receptor Is a Novel Target for Improving Cold Preservation in Rodent Kidney Transplants, International Journal of Molecular Sciences 2023, **IF=4.9**

Other Publications

Tamas Lakat, Andrea Fekete, Kornel Demeter, **Akos R Toth**, Zoltan K Varga, Attila Patonai, Hanga Kelemen, Andras Budai, Miklos Szabo, Attila J Szabo, Kai Kaila, Adam Denes, Eva Mikics, Adam Hosszu; Perinatal asphyxia leads to acute kidney damage and increased renal susceptibility in adulthood, American Journal of Physiology-Renal Physiology 2024, **IF=3.4**

Dora B Balogh, Agnes Molnar, Arianna Degi, **Akos Toth**, Lilla Lenart, Adar Saeed, Adrienn Barczi, Attila J Szabo, Laszlo J Wagner, Gyorgy Reusz, Andrea Fekete; Cardioprotective and antifibrotic effects of low-dose renin–angiotensin–aldosterone system inhibitors in type 1 diabetic rat model, International Journal of Molecular Sciences 2023, **IF=4.9**

IE Vlad, C Martin, **AR Toth**, J Papp, SD Anghel; Bacterial inhibition effect of plasma activated water, Romanian Reports in Physics 2019; **IF=2.147**

10. Acknowledgements

First and foremost, I would like to thank my supervisor, Adam Hosszu, for his personal and professional support. I am particularly thankful for his invaluable guidance in improving my scientific writing and for his mentorship in understanding and conducting academic research.

I would like to express my deep sense of gratitude to Prof. Andrea Fekete for giving me the opportunity to be part of MTA-SE Lendület "Momentum" Diabetes Research Group and for continuously supporting me even in the hard times. Her exceptional dedication and encouragement were a constant source of motivation and greatly contributed to my perseverance and professional development.

Furthermore, I would like to deeply appreciate Prof. Attila Szabó for his approval of my application during my PhD study at Pediatric Center, Semmelweis University.

I am also very grateful to Judit Hodrea, post-doc of our group, for her kind and supportive attitude since I joined the laboratory, as well as for her valuable guidance and advice throughout my work.

I would like to thank all my colleagues in the lab for creating a motivating and supportive working environment. I am especially grateful to Tamas Lakat, Timea Medveczki, Agnes Molnar, Eszter Levai and Csenge Pajtok for the insightful scientific discussions and the many enjoyable moments we shared. Their continuous support and professional contributions were essential to the completion of this work. I am grateful to Dora Bianka Balogh, former post-doc for her help and advice during our joint work. I could not be more thankful to Maria Bernath for help with the laboratory work and for her kind attention on everyone in the lab. I am privileged and glad of having the fellow and former colleagues as well: Alexandra Rozsahegyi, Zsuzsanna Buzogany, Lilla Szecsi, Luca Reicher, Hanga Kallay, Valeria Scheffer, Adar Amedi, Minh Tran, Eva Forizs, Lilla Lenart, Apor Veres-Szekely, Beata Szebeni, Domonkos Pap, Csenge Szasz, Peter Bokrossy, Magdolna Keszthelyi.

Last but not least, I am deeply grateful to my wife and to my entire family for their unwavering love, patience, and support throughout these years. Thank you for believing in me, encouraging me at every step, and giving me the strength to pursue my goals. I could not have completed this work without you.